



LARGE-SCALE BIOLOGY ARTICLE

A PXY-Mediated Transcriptional Network Integrates Signaling Mechanisms to Control Vascular Development in Arabidopsis^[OPEN]

Margot E. Smit,^{a,b,1,2} Shauni R. McGregor,^{c,1,3} Heng Sun,^d Catherine Gough,^c Anne-Maarit Bågman,^a Cara L. Soyars,^{e,4} Johannes T. Kroon,^c Allison Gaudinier,^{a,5} Clara J. Williams,^{a,6} Xiyan Yang,^d Zachary L. Nimchuk,^e Dolf Weijers,^b Simon R. Turner,^f Siobhán M. Brady,^{a,7} and J. Peter Etchells^{a,c,7}

^a Department of Plant Biology and Genome Center, University of California, Davis, California 95616

^b Laboratory of Biochemistry, Wageningen University, 6708 WE, Wageningen, The Netherlands

^c Department of Biosciences, Durham University, Durham DH1 3LE, United Kingdom

^d National Key Laboratory of Crop Genetic Improvement, Huazhong Agricultural University, Wuhan, Hubei 430070, China

^e Department of Biology, University of North Carolina, Chapel Hill, North Carolina 27599

^f School of Biological Science, University of Manchester, Manchester, M13 9PT, United Kingdom

ORCID IDs: 0000-0001-8285-5130 (M.E.S.); 0000-0002-6818-362X (S.M.); 0000-0002-5790-0662 (H.S.); 0000-0003-2459-9022 (C.G.); 0000-0002-7586-8184 (A.-M.B.); 0000-0002-2713-5146 (C.L.S.); 0000-0003-2086-6074 (J.T.K.); 0000-0002-4350-6760 (A.G.); 0000-0003-1292-6313 (C.J.W.); 0000-0003-1305-8677 (X.Y.); 0000-0003-1826-0671 (Z.L.N.); 0000-0003-4378-141X (D.W.); 0000-0003-4859-1068 (S.R.T.); 0000-0001-9424-8055 (S.M.B.); 0000-0002-8524-4949 (J.P.E.)

The cambium and procambium generate the majority of biomass in vascular plants. These meristems constitute a bifacial stem cell population from which xylem and phloem are specified on opposing sides by positional signals. The PHLOEM INTERCALATED WITH XYLEM (PXY) receptor kinase promotes vascular cell division and organization. However, how these functions are specified and integrated is unknown. Here, we mapped a putative PXY-mediated transcriptional regulatory network comprising 690 transcription factor-promoter interactions in Arabidopsis (*Arabidopsis thaliana*). Among these interactions was a feedforward loop containing transcription factors WUSCHEL HOMEBOX RELATED14 (WOX14) and TARGET OF MONOPTEROS6 (TMO6), each of which regulates the expression of the gene encoding a third transcription factor, LATERAL ORGAN BOUNDARIES DOMAIN4 (LBD4). PXY signaling in turn regulates the WOX14, TMO6, and LBD4 feedforward loop to control vascular proliferation. Genetic interaction between LBD4 and PXY suggests that LBD4 marks the phloem-procambium boundary, thus defining the shape of the vascular bundle. These data collectively support a mechanism that influences the recruitment of cells into the phloem lineage, and they define the role of PXY signaling in this context in determining the arrangement of vascular tissue.

INTRODUCTION

In vascular plants, water is taken up from the soil but sugars are assimilated in leaves, so the movement of these resources throughout the plant body is essential for plant survival. Xylem and phloem are the specialized vascular tissues that perform this function. Both arise in a highly ordered manner from meristematic divisions in the cambium and procambium. Multiple mechanisms have been identified that influence vascular development (Fischer et al., 2019); however, how these mechanisms interact to coordinate vascular morphogenesis is poorly understood.

Auxin is central to vascular tissue specification, and its responses are mediated by, among others, *MONOPTEROS* (*MP*), which encodes an Auxin Response Factor (Hardtke and Berleth, 1998). *Arabidopsis* (*Arabidopsis thaliana*) *mp* mutants are characterized by patterning defects in the embryo vascular cylinder (Berleth and Jurgens, 1993). *MP* is thought to act as an activator of vascular proliferation in seedlings (Vera-Sirera et al., 2015) or as a repressor of vascular proliferation in mature plant tissues (Mattsson et al., 2003; Brackmann et al., 2018). With additional signals, *MP* controls two pathways that stimulate vascular

¹ These authors contributed equally to this work.

² Current address: Department of Biology, Stanford University, Stanford, California 94305

³ Current address: Department of Animal and Plant Sciences, University of Sheffield, Western Bank, Sheffield, S10 2TN, United Kingdom

⁴ Current address: Thermo Fisher Scientific, Carlsbad, California 92008

⁵ Current address: Department of Plant and Microbial Biology, University of California, Berkeley, California 94720

⁶ Current address: Ghent University, Vlaams Instituut voor Biotechnologie, Department of Plant Systems Biology, 9052 Ghent, Belgium.

⁷ Address correspondence to sbrady@ucdavis.edu and peter.etchells@durham.ac.uk.

The authors responsible for distribution of materials integral to the findings presented in this article in accordance with the policy described in the Instructions for Authors (www.plantcell.org) are: Siobhán M. Brady (sbrady@ucdavis.edu) and J. Peter Etchells (peter.etchells@durham.ac.uk).

^[OPEN] Articles can be viewed without a subscription.

www.plantcell.org/cgi/doi/10.1105/tpc.19.00562

IN A NUTSHELL

Background: Vascular tissues transport water, salts, and photosynthates within the plant body. The xylem moves water and salts from the roots up, and the phloem distributes water and sugars throughout the plant. As the plant grows, the stem grows thicker in part because the woody vascular tissues expand. Between the xylem and phloem are stem cells that divide and develop into xylem and phloem. These divisions increase vascular tissue size and provide structural support to the plant. Due to the importance of vascular tissues, both the divisions and fate of stem cells must be tightly controlled. Several proteins have been found to control cell division rate or xylem/phloem fate in vascular stem cells.

Question: PXY controls vascular stem cell division rate but is also needed to organize xylem and phloem into two separate domains. However, we don't know how PXY can control these two separate processes. Our goal was to identify genetic interactions that help explain the role of PXY.

Findings: We looked at the transcriptional regulation of vascular genes in *Arabidopsis thaliana*. We identified interactions between DNA-binding proteins and regulatory DNA sequences using enhanced Yeast One Hybrid assays. We constructed a potential transcriptional regulatory network from the 690 interactions. The network contains an interesting feed-forward loop controlled by PXY. In our network, *LBD4* is regulated by both *WOX14* and *TMO6*, but *WOX14* also regulates *TMO6*. As a result, *WOX14* influences *LBD4* in two ways: directly and indirectly via *TMO6*. We studied the genetic interactions between these components and found that PXY regulates the components of this feed-forward loop to control vascular stem cell divisions. In addition, PXY regulation of *LBD4* marks the boundary between stem cells and phloem cells. Thus, we identified genetic mechanisms used by PXY to regulate both division rate and fate separation.

Next steps: The challenges are to understand how network interactions change in a cell-type specific manner through development and to identify interactions that have been modified through evolution. Wood is an important biomaterial and carbon sink. Our network provides a basis for experiments aimed at modifying plants to maximize wood formation.

proliferation. The first pathway is characterized by *TARGET OF MONOPTEROS5* (*TMO5*), encoding a basic helix-loop-helix (bHLH) transcription factor (Schlereth et al., 2010) that with its homologs promotes cell divisions in the vascular cylinder. These transcription factor genes are upregulated by MP in the embryo. *TMO5*-like proteins perform this function in heterodimers with a second class of bHLH transcription factors including *LONESOME HIGHWAY* and its relatives (Ohashi-Ito and Bergmann, 2007; De Rybel et al., 2013, 2014; Ohashi-Ito et al., 2014; Vera-Sirera et al., 2015). The second pathway targeted by MP involves auxin-responsive *TMO6* (Schlereth et al., 2010), which encodes a member of the *DOF* family of transcription factors. Multiple members of the *DOF* family have been shown to promote vascular cell divisions (Guo et al., 2009; Waki et al., 2013; Konishi et al., 2015; Miyashima et al., 2019; Smet et al., 2019). The expression of a subset of *DOF* genes, including *TMO6*, is also controlled by cytokinin (Miyashima et al., 2019). Thus, *TMO6* responds to both cytokinin and auxin.

TRACHEARY ELEMENT DIFFERENTIATION INHIBITORY FACTOR (TDIF) and PHLOEM INTERCALATED WITH XYLEM/TDIF RECEPTOR (PXY/TDR; referred to hereafter as PXY) are a ligand-receptor pair (Hirakawa et al., 2008; Morita et al., 2016; Zhang et al., 2016) that also promote cell division in vascular meristems. The TDIF peptide is derived from *CLE41*, *CLE42*, and *CLE44*. These genes are expressed in the phloem while PXY is expressed in the procambium (Ito et al., 2006; Fisher and Turner, 2007; Hirakawa et al., 2008; Etchells and Turner, 2010). Upon TDIF binding to the PXY receptor, the transcription factor genes *WUSCHEL HOMEODOMAIN RELATED4* (*WOX4*), *WOX14*, and *ATHB8* are upregulated (Hirakawa et al., 2010; Etchells et al., 2013). Another transcription factor, *BES1*, is also regulated by TDIF-PXY.

When TDIF binds to PXY, an interaction between PXY and GSK3 kinases results in the phosphorylation and degradation of *BES1*. *BES1* is thought to promote xylem differentiation, so its degradation preserves cambium pluripotency (Kondo et al., 2014).

Interactions between TDIF-PXY and auxin signaling contribute to vascular tissue development (Suer et al., 2011; Smetana et al., 2019). Both auxin and PXY responses are mediated by interactions with GSK3 signaling proteins. The GSK3, BIN2-LIKE 1 regulates the auxin response via phosphorylation of MP, and during vascular development, this requires the absence of active TDIF-PXY complexes (Cho et al., 2014; Kondo et al., 2014; Han et al., 2018). Auxin also induces the expression of the TDIF-PXY targets *ATHB8* and *WOX4* (Baima et al., 1995; Mattsson et al., 2003; Suer et al., 2011). The induction of *TMO5-like1* (*T5L1*) and *LHW* also increases *ATHB8* expression (Vera-Sirera et al., 2015). *ATHB8* encodes an HD-Zip III transcription factor (Baima et al., 2001) whose paralogues modulate the expression of auxin biosynthesis and auxin perception genes (Müller et al., 2016). *HD-Zip III* genes have wide-ranging roles in vascular patterning and proliferation (Zhong and Ye, 1999; Emery et al., 2003; Prigge et al., 2005; Carlsbecker et al., 2010; Baima et al., 2014; Ramachandran et al., 2016).

In addition to PXY, a second family of receptor kinases, members of the *ERECTA* (*ER*) family, control vascular expansion in *Arabidopsis* (Ragni et al., 2011; Uchida et al., 2012; Uchida and Tasaka, 2013; Ikematsu et al., 2017). PXY and its paralogues genetically interact with *ER* family members to control cell proliferation, cell size, and cell type organization in vascular tissues (Etchells et al., 2013; Uchida and Tasaka, 2013; Wang et al., 2019). *ER* also interacts with auxin signaling components and members of the *HD-Zip III* family in

developmental contexts that include meristem maintenance, stem architecture, and leaf development (Woodward et al., 2005; Chen et al., 2013). Thus, interactions between *PXY*, auxin, cytokinin, *HD-Zip III*s, *ER*, and *GSK3*s constitute a significant proportion of the regulatory mechanisms that define how vascular tissue develops.

How do these and other factors combine to coordinate vascular development at the level of transcription? Here, to provide a framework for answering this question, we generated a transcriptional regulatory network (TRN) incorporating a significant proportion of known regulators of vascular development in Arabidopsis. We used high-throughput enhanced yeast one-hybrid (eY1H) assays (Gaudinier et al., 2011, 2017; Reece-Hoyes et al., 2011) to identify transcription factors that bind to the promoters of vascular regulators. Our vascular development TRN comprises 690 transcription factor-promoter interactions. To demonstrate the power of our network to identify novel regulators and interactions, we characterized a feed-forward loop incorporating three transcription factors that link auxin and PXY-mediated signaling: *WOX14*, *TMO6*, and *LATERAL ORGAN BOUNDARIES DOMAIN4* (*LBD4*). Feed-forward loops are often involved in dynamic gene regulation (Mangan and Alon, 2003), and our results demonstrate that, in response to auxin and TDIF-PXY signaling, the genes within this circuit define a zone of procambial activity to maintain the arrangement of vascular tissue of the stem.

RESULTS

Identification of Putative TDIF Target Genes

To generate a TRN downstream of TDIF, we first identified putative TDIF target genes. The TDIF peptide ligand is derived from *CLE41*, *CLE42*, and *CLE44* proteins, so we compared the transcriptomes of mature (5-week-old) stem bases of *35S:CLE41* lines (i.e., increased PXY signaling) with that of the wild type. Genes were considered differentially expressed where the *P* value, adjusted for multiple hypothesis testing, was ≤ 0.05 (Supplemental Data Set 1). *35S:CLE41* plants had on average 100.7 ± 9.1 undifferentiated cells per vascular bundle compared with 59.5 ± 5.5 in the wild type (Supplemental Figures 1A and 1B). Consistent with the vascular overproliferation phenotype, genes shown to be predominantly expressed in the procambium, including *BRI-LIKE1*, *PINFORMED1*, and *MP* (Gälweiler et al., 1998; Hardtke and Berleth, 1998; Caño-Delgado et al., 2004), demonstrated significant increases in expression in *35S:CLE41* plants relative to the wild type (Supplemental Table 1). The expression levels of previously described targets of PXY signaling, *ATHB8* and *WOX14* (Hirakawa et al., 2010; Etchells et al., 2013), increased 2.78-fold ($P < 0.001$) and 4.76-fold, respectively, in *35S:CLE41* versus the wild type ($P < 0.001$). Our microarray data were further validated using qRT-PCR of a select number of genes involved in xylem cell differentiation or transcriptional regulation, including an *ASPARTIC PEPTIDASE* gene, *GMC OXIDOREDUCTASE*, *MAP70-5*, *IAA30*, and *MYB38* (Supplemental Figure 1C), and were consequently used to guide promoter selection for eY1H experiments.

A PXY-Mediated Transcriptional Network for Vascular Development

To understand how factors that control PXY-mediated vascular development interact, and to identify novel vascular regulators, we identified transcription factor-promoter interactions using eY1H assays (Gaudinier et al., 2011; Reece-Hoyes et al., 2011). Bait were selected as promoters from five groups of genes representing factors that regulate PXY-mediated or xylem cell development in the inflorescence stem (Supplemental Table 2). Group I included *PXY* and *PXL* receptors (Fisher and Turner, 2007), ligands (Ito et al., 2006), and their target transcription factor gene, *WOX14* (Etchells et al., 2013). Group II comprised *GSK3* family members, which interact with the PXY kinase domain (Kondo et al., 2014) and their target transcription factor genes *BES1* and *BZR1* (He et al., 2002). The *ER* family of receptors were included in group II, as ER family receptors act in part through *GSK3* signaling (Kim et al., 2012), and they genetically interact with PXY family receptors (Wang et al., 2019). Genes involved in auxin or cytokinin perception and auxin responses that also demonstrated differential expression in *35S:CLE41* constituted groups III and IV. These included *TMO6*, a transcriptional target of MP (Schlereth et al., 2010), and its paralogue *DOF1.8* (Supplemental Table 2; Le Hir and Bellini, 2013). Promoters of *HD-Zip III* transcription factor genes that were differentially expressed in *35S:CLE41* lines and have been shown elsewhere to control vascular development (Zhong and Ye, 1999; Baima et al., 2001; McConnell et al., 2001; Emery et al., 2003; Carlsbecker et al., 2010; Müller et al., 2016) were used as bait for group V. Finally, based on very high expression in *35S:CLE41*, *LBD4/ASL6*, and its homolog, *LBD3/ASL9*, genes of unknown function were identified (Supplemental Table 2).

We screened these promoters against a collection of 812 root-expressed transcription factors that represent more than 95% of the transcription factors with enriched expression in the Arabidopsis stele (Gaudinier et al., 2011; Taylor-Teeple et al., 2015). The resulting interactions comprise a network consisting of 312 nodes (Figure 1A). Each node represents a gene either as a promoter, as a transcription factor, or as both. The nodes were connected by 690 edges, each representing a transcription factor binding to a promoter, as identified in the eY1H assays (Figure 1A; Supplemental Data Set 2). To visualize the nodes and edges, we designed a custom layout in Cytoscape (Shannon et al., 2003). Promoter nodes were colored and arranged in the five association groups described in the previous paragraph: PXY signaling (group I; blue), ER/BRI1/GSK3 signaling (group II; mint), auxin/cytokinin perception (group III; green/red), targets of MP and affiliates (group IV; orange/purple), and HD-Zip IIIs (group V; olive; Figure 1A). Transcription factors were colored white and positioned in the network based on their target profiles. Those targeting similar sets of genes/groups were placed together. Transcription factors interacting with promoters in more than two groups were placed at the center of the network. Those interacting with one or two promoter groups were placed on the periphery. In total, 287 transcription factors targeted at least one promoter in the network. The transcription factor families with the greatest representation were AP2/EREBP transcription factors, of which 46 members interacted with the screened promoters, followed by MYB (40

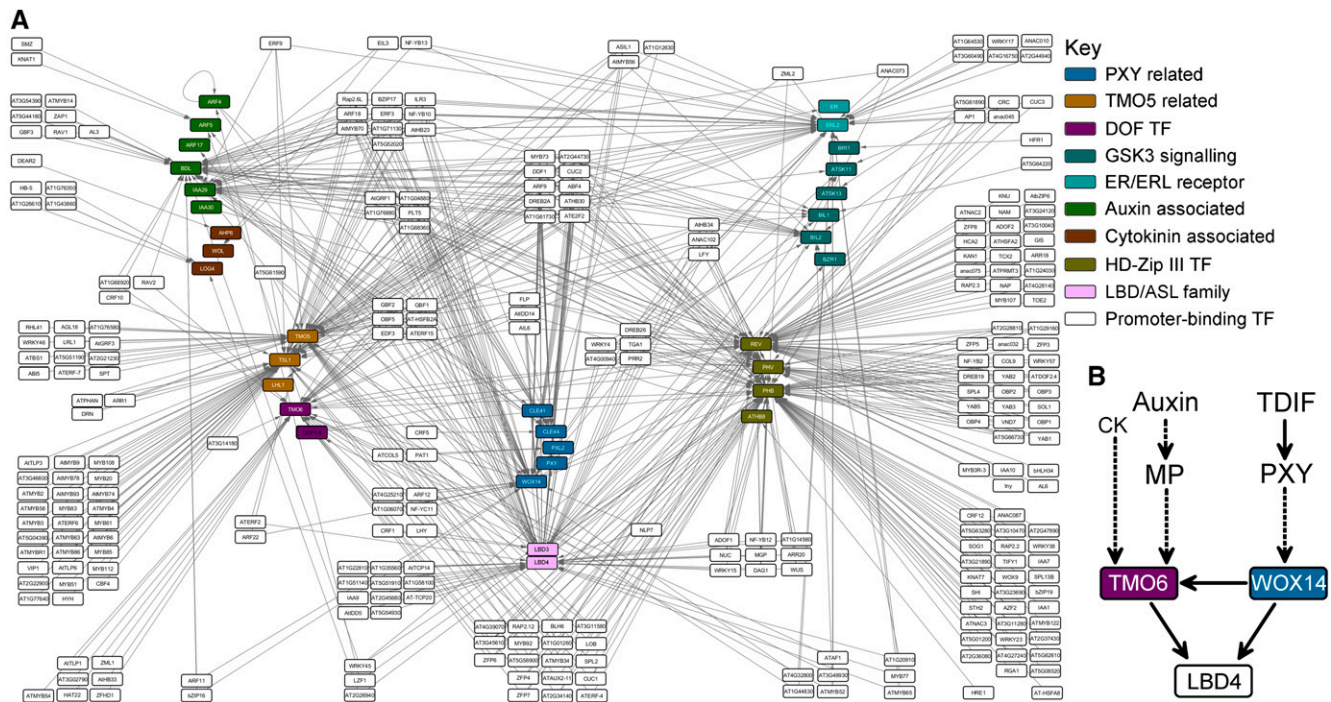


Figure 1. Diagrammatic Representation of the Vascular Development TRN.

(A) Representation of all the interactions identified using eY1H. Promoters screened are shown as colored nodes. Transcription factors are shown as white nodes. Gray lines connect transcription factor nodes, with promoter nodes representing interactions in eY1H assays.

(B) Subnetwork describing the feed-forward loop constituted of WOX14, TMO6, and LBD4 interactions and its regulation by auxin, cytokinin (CK), and TDIF-PXY signaling.

interactors), and C2H2 transcription factors (31 interactors). A list of all interacting transcription factors and their respective classes is shown in Supplemental Data Set 3.

We predicted that the network would be enriched for genes differentially expressed in *35S:CLE41* (Supplemental Figure 2A). A significant enrichment ($P = 2.2e-6$) was observed using Fisher's exact test. Furthermore, using previously described loss-of-function gene expression data from *pxy* mutants (Etchells et al., 2012), a more dramatic enrichment ($P = 1.57e-62$; Supplemental Figure 2B) was observed. Thus, the network represents a PXY-mediated TRN.

A WOX14-Mediated Feed-Forward Loop

We used our predicted vascular development network (Figure 1A) combined with our *35S:CLE41* transcriptome data (Supplemental Data Set 1) to identify a regulatory circuit for further analysis. Promoters were ranked by the number of transcription factors that bound to them (in-degree binding). *PHB*, *PHV*, *LBD4*, and *T5L1* demonstrated the highest levels of in-degree connectivity in our TRN (Supplemental Data Set 4). In addition to its high in-degree value of 68 (ranked third), *LBD4* also demonstrated an 11-fold increase in expression in *35S:CLE41* versus the wild type (Supplemental Table 1; Supplemental Data Set 1), higher than that of any other transcription factor. Furthermore, its function had not previously

been described, making it a strong candidate for further investigation.

TMO6 and *WOX14* were predicted to bind to and regulate *LBD4* (Figure 1B; Supplemental Data Set 2). Both were also expressed to a high degree in *35S:CLE41* lines, each demonstrating a 4.8-fold increase in expression (Supplemental Table 2; Supplemental Data Set 1). *WOX14* was also predicted to bind to and regulate both *TMO6* and *LBD4* (Figure 1B; Supplemental Data Set 2); thus, these three transcription factors were present in a feedforward loop (Figure 1B). Feedforward loops are enriched within xylem regulatory networks (Taylor-Teeples et al., 2015) and ensure robust regulation of their target genes (Shen-Orr et al., 2002; Mangan and Alon, 2003; Kalir et al., 2005; Kaplan et al., 2008). We hypothesized that the *WOX14-TMO6-LBD4* feed-forward loop plays a key role in regulating vascular development due to its potential to integrate auxin, cytokinin, and TDIF-PXY signaling (Figures 1A and 1B). Specifically, *TMO6* is transcriptionally regulated by both auxin (Schlereth et al., 2010) and cytokinin (Miyashima et al., 2019; Smet et al., 2019). *WOX14* is regulated by TDIF-PXY (Etchells et al., 2013). Consequently, based on high network connectivity and high expression in *35S:CLE41* relative to the wild type, their likelihood of integrating PXY, auxin, and cytokinin signaling, and their arrangement in a feedforward loop, we selected the regulatory circuit involving *TMO6*, *WOX14*, and *LBD4* for further study.

Genetic Elimination of the *TMO6-WOX14-LBD4* Feedforward Loop

To determine the significance of the *TMO6-WOX14-LBD4* feedforward loop in vascular development, we genetically perturbed each of these genes singly and in combination. We combined *wox14* (Etchells et al., 2013) and *lbd4* Arabidopsis T-DNA lines with *tmo6* mutants generated by genome editing. The single mutants demonstrated no changes in the number of cells per vascular bundle or vascular morphology compared with the wild type (Figures 2A, 2F, 2G, 3G, 3J, and 3K; Supplemental Figures 3A, 3B, and 3E–3G; Etchells et al., 2013). By contrast, the number of cells present per vascular bundle was significantly reduced in *tmo6 wox14 lbd4* triple and *tmo6 wox14* double mutant stems ($P < 0.002$ and $P = 0.002$; Figures 2A–2F; Supplemental Data Set 5). Consistent with *TMO6* and *WOX14* acting as upstream regulators of *LBD4*, as predicted from the eY1H data (Figure 1A), the *tmo6 wox14* and *tmo6 wox14 lbd4* lines were indistinguishable ($P = 0.371$; Figures 2D to 2F).

In the wild type, vascular bundles expand to a greater degree along the radial axis of the stem than the tangential, and thus vascular bundle shape can be measured by comparing tangential:radial ratios. In the *tmo6 wox14 lbd4* lines, this ratio was higher than in the wild type (Figure 2G), and as such, the triple mutant demonstrated reduced expansion along the radial axis of the stem. This genetic interaction supports the idea that the feedforward loop transcription factors are components of the same pathway and that they are critical for controlling vascular proliferation and shape.

WOX14 and *TMO6* Are Sufficient to Regulate Gene Expression within the Feedforward Loop in Plant Cells

A prerequisite for in planta transcriptional regulation within the feedforward loop is the expression of *TMO6*, *WOX14*, and *LBD4* in the same place and time. Using in situ hybridization, *TMO6* and *LBD4* mRNA antisense probes hybridized to cells in the vascular tissue of the inflorescence stem, with expression maxima at the phloem-procambium boundary (Figures 3A and 3B; Supplemental Figure 4A for sense controls). *WOX14:GUS* expression (Figure 3C) was also present in phloem-procambium boundary cells, in addition to other vascular cell types, as described previously described by Etchells et al. (2013).

Given the genetic interaction and overlapping expression of *TMO6*, *WOX14*, and *LBD4*, we sought more direct evidence for the feedforward loop interactions identified in the eY1H in planta. We transformed wild tobacco (*Nicotiana benthamiana*) leaf protoplasts with a construct that harbored *LBD4pro:LUC* (*LUCIFERASE*) and *35S:REN* (*RENILLA*) cassettes and determined *LBD4pro* activity as LUC activity normalized to that of *REN*. LUC activity was higher in cells co-transformed with both *LBD4pro:LUC* reporter and a *35S:TMO6* construct than in cells transformed with the *LBD4pro:LUC* reporter and a control (empty vector) construct ($P < 0.001$; Supplemental Figure 5A). *LBD4* promoter activity further increased ($P = 0.005$) when cells were co-transformed with *LBD4pro:LUC*, *35S:TMO6*, and *35S:WOX14*. The LUC activity in cells containing both *LBD4pro:LUC* and *35S:*

WOX14 was similar to that in cells harboring *LBD4pro:LUC* and an empty vector control.

We used a similar strategy to verify *WOX14*-mediated regulation of transcripts under the control of the *TMO6* promoter. Here, LUC activity was significantly higher ($P < 0.001$) when *TMO6pro:LUC* was co-transformed with a *35S:WOX14* construct than when transformed with a control construct (Supplemental Figure 5B). In summary, these multiple pieces of data provide evidence that the *WOX14-TMO6-LBD4* transcription factor-promoter interactions are sufficient to regulate transcription in plant cells (Supplemental Figure 5).

Interconnected Transcriptional Regulation in the Feedforward Loop

We obtained in planta genetic evidence for these regulatory relationships by performing qRT-PCR and examining loss-of-function mutant alleles. Our network suggested that *LBD4* and *TMO6* act downstream of *WOX14* (Figure 1B), so we tested the expression levels of these genes in *wox14* mutants in the basal one-third of 15-cm inflorescence stems, where *WOX14* expression had previously been shown to be the highest. Because *WOX14* acts redundantly with *WOX4* (Etchells et al., 2013), *wox4* and *wox4 wox14* lines were also included in our analysis. Consistent with the notion that *WOX14* regulates *TMO6* and *LBD4* expression, *wox14* stems exhibited lower levels of *TMO6* and *LBD4* expression than the wild type (Figures 3D and 3E). Thus, wild-type levels of *TMO6* and *LBD4* expression are dependent on the expression of *WOX14*. Further reductions in *TMO6* and *LBD4* expression were not observed in *wox4 wox14* lines relative to single *wox4* or *wox14* mutant alleles.

To determine if *LBD4* expression is also dependent on *TMO6* expression (Figure 1B), we tested *tmo6* mutant lines. In the basal one-half of 15-cm inflorescence stems, *LBD4* expression was unchanged in *tmo6* relative to the wild type (Figure 3F; Supplemental Table 3). We reasoned that the dependency of *LBD4* on *TMO6* might be revealed in a sensitized genetic background. To test this hypothesis, we generated *wox4 wox14 tmo6* and *pxy pxl1 pxl2 tmo6* (*pxf tmo6*) lines. *tmo6* dramatically enhanced the cell division defect observed in the *pxf* triple mutants (Figures 3G–3J; Supplemental Data Set 5), although the shapes of the bundles (based on the tangential:radial ratio) did not differ from those of the *pxf* lines (Figure 3K). We measured *LBD4* expression in the lower halves of inflorescence stems. The reductions in *LBD4* expression in both the *pxf* and *wox4 wox14* lines proved not to be significant ($P = 0.167$ and $P = 0.102$; Figure 3F; Supplemental Table 3). By contrast, *LBD4* expression was significantly lower in the *pxf tmo6* and *wox4 wox14 tmo6* mutants relative to the wild type ($P = 0.031$ and $P = 0.027$). Thus, while *LBD4* expression did not depend on the presence of *TMO6* in the lower halves of 15-cm inflorescence stems, the reduced expression was exacerbated in *tmo6 pxf* and *tmo6 wox4 wox14* relative to the parental lines (Figure 3F). Therefore, *TMO6*, redundantly with *TDIF/PXY* signaling, regulates *LBD4* expression.

While these results supported the idea that *TMO6* and *WOX14* regulate *LBD4* expression, they also raised the question of why

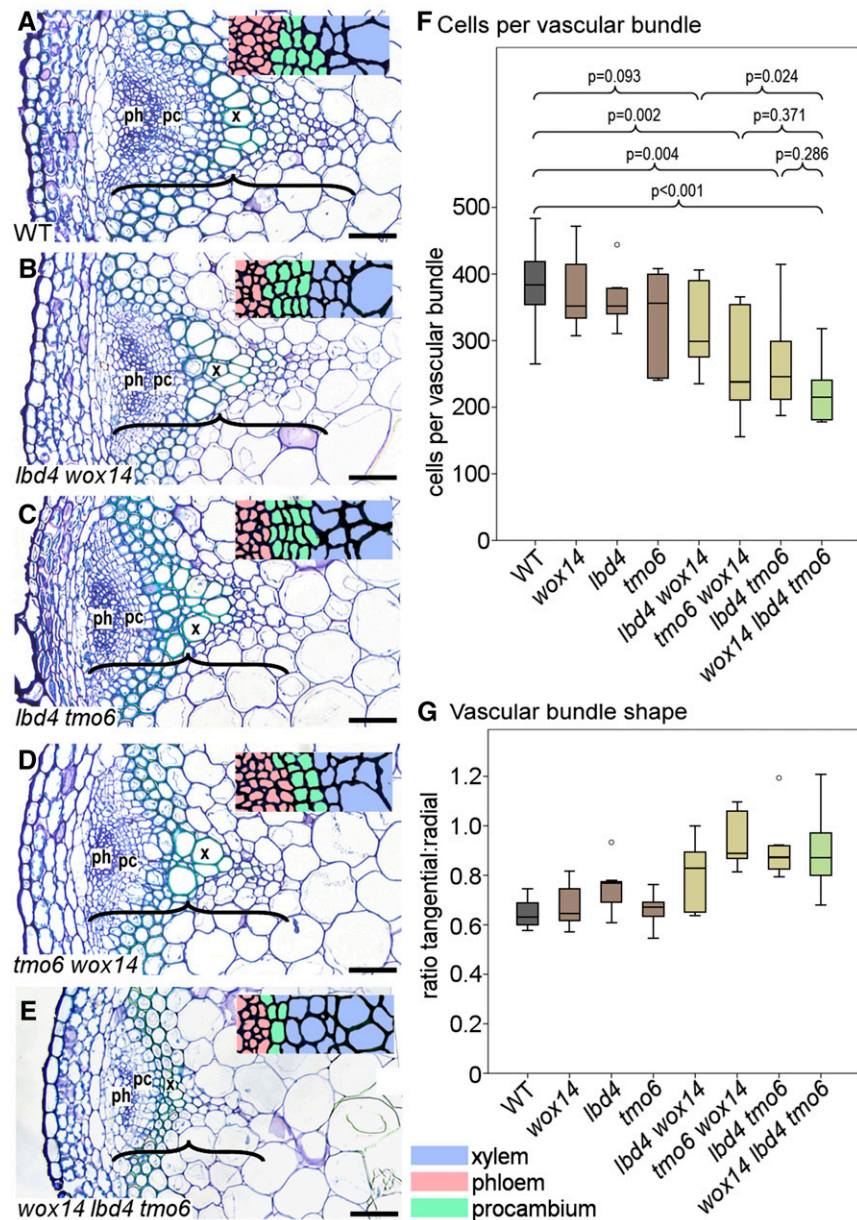


Figure 2. Consequences of Removing the Feed-Forward Loop.

(A) to (E) Morphology of vascular bundles from inflorescence stems in the wild type **(A)**, *lbd4 wox14* **(B)**, *lbd4 tmo6* **(C)**, *tmo6 wox14* **(D)**, and *wox14 lbd4 tmo6* **(E)**. Transverse sections were stained with toluidine blue. Insets show closeups of the cambium (green). pc, cambium; ph, phloem; x, xylem. Brackets mark the vascular bundle size along the radial axis of the stem. Bars = 50 μ m.

(F) Boxplots showing mean number of cells per vascular bundle in *wox14 lbd4 tmo6* and double and single mutant controls. Significant differences were determined by ANOVA with an LSD posthoc test ($n = 6$).

(G) Boxplot showing vascular bundle shape determined by measuring the ratio of tangential to radial axis ($n = 6$).

Boxplots show median (inner line) and inner quartiles (box). Whiskers extend to the highest and lowest values no greater than 1.5 times the inner quartile range, and circles show outliers.

LBD4 expression was reduced in *wox4 wox14* lines when the lower one-third of 15-cm inflorescence stems was sampled (Figure 3E) but not when the lower one-half was sampled (Figure 3F). We reasoned that *LBD4* expression may vary along the apical-basal axis of the stem and tested this hypothesis using

qRT-PCR. *LBD4* expression was significantly higher in the basal one-third of the inflorescence stem relative to the middle or apical sections (Supplemental Figure 4B), which is consistent with the *LBD4* expression levels observed in Figures 3E and 3F.

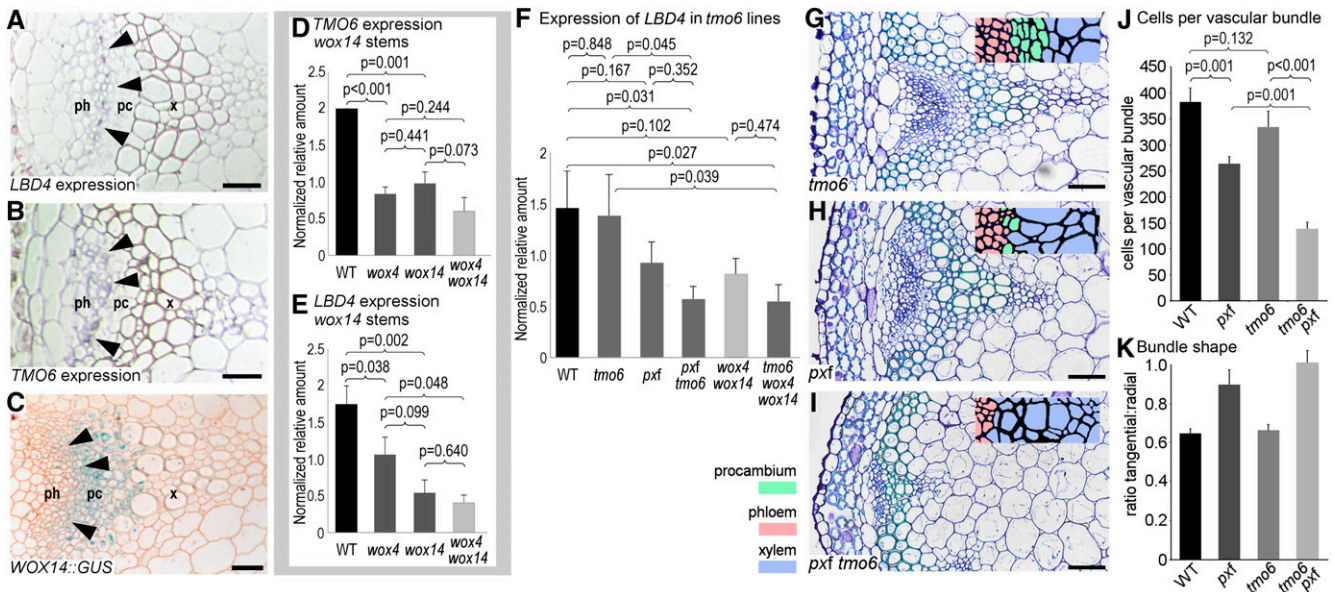


Figure 3. Gene Expression Studies Supporting a Regulatory Relationship between *WOX14*, *TMO6*, and *LBD4*.

(A) to (C) *WOX14*, *TMO6*, and *LBD4* demonstrate overlapping expression in inflorescence stem vascular bundles. Antisense probes against *LBD4* mRNA (A) or *TMO6* mRNA (B) localize to the phloem-procambium boundary. A *WOX14::GUS* transcriptional fusion (C) shows the presence of broad *WOX14* expression in vascular bundles including at the phloem-procambium boundary. pc, cambium; ph, phloem; x, xylem. Bars = 30 μ m. (D) and (E) qRT-PCR on inflorescence stem tissue from the lower third of the stem showing that *TMO6* (D) and *LBD4* (E) expression is dependent on *WOX14*. (F) qRT-PCR showing that *TMO6* and *Pxf* are required to maintain *LBD4* expression in the lower one-half of 15-cm inflorescence stems. Expression differences were determined in technical triplicate for each of three biological replicates. Tissue for each biological replicate was taken from a different pot. Statistical differences were determined with ANOVA and an LSD posthoc test ($n = 3$ biological replicates; error bars are SE). (G) to (I) Vascular bundles from the inflorescence stems of *tmo6* (G), *pxf* (H), and *pxf tmo6* (I) plants. Transverse sections were stained with toluidine blue. Bars = 30 μ m. (J) Graph showing the mean number of cells per vascular bundle. P values were determined with ANOVA and an LSD posthoc test. (K) Histogram showing vascular bundle shape determined by measuring the ratio of tangential to radial axis. ($n = 6$; error bars are SE).

TDIF-PXY Dynamically Regulates the Feedforward Loop

As *LBD4* expression was reduced in the *pxf tmo6* background and *tmo6* genetically enhanced the *pxf* phenotype (Figures 3I–3K), we further explored the expression of genes in this feedforward loop in response to perturbations in TDIF-PXY signaling. We measured *LBD4* and *TMO6* expression in *pxf* (Fisher and Turner, 2007; Wang et al., 2019) and in *cle41 cle42 cle43 cle44* mutants (referred to hereafter as *tdif*; Supplemental Figure 6), which were generated by genome editing. Here, we measured gene expression in the lower one-third of 10-cm stems. A significant reduction in *LBD4* expression was not observed, but reduced *TMO6* expression was observed (Figures 4A and 4B). These results demonstrate that *TMO6* is responsive to genetic perturbation of TDIF-PXY signaling.

To determine the temporal dynamics of gene regulation within the feedforward loop, we applied TDIF or control peptide to 5-d-old wild type, *pxy*, and *wox4 wox14* seedlings. *WOX14* expression increases upon TDIF application (Etchells et al., 2013). Similarly, a 2-h treatment with 5 μ M TDIF in wild-type plants resulted in increased *LBD4* and *TMO6* expression relative to plants treated with a P9A negative control (Figures 4C and 4D). This induction of *TMO6* and *LBD4* was absent, and their expression was even further reduced, in *pxy* and *wox4 wox14* mutants, suggesting that

PXY/TDIF activate the expression of all genes within the feedforward loop (Figures 4A to 4D).

The WOX14-TMO6-LBD4 Feedforward Loop Is Auxin Responsive

MP is a transcriptional regulator of *TMO6* (Schlereth et al., 2010), and crosstalk between auxin and TDIF-PXY signaling has been described (Suer et al., 2011; Han et al., 2018). We therefore tested the expression of all three transcription factors in the feedforward loop upon exposure to 10 μ M IAA. *TMO6* and *LBD4* expression increased in response to a 6-h auxin treatment in both the wild type and *wox14* mutants, demonstrating that auxin regulates *LBD4* and *TMO6* expression in a *WOX14*-independent manner (Figures 4E and 4F). *WOX14* was also upregulated in response to auxin treatment (Figure 4G).

LBD4 Regulates Vascular Cell Number and Organization

To determine the function of this feedforward loop in vascular development, we characterized vascular development in inflorescence stems upon genetic perturbation of the final gene within the feedforward loop, *LBD4*. The phenotype of the *lbd4*

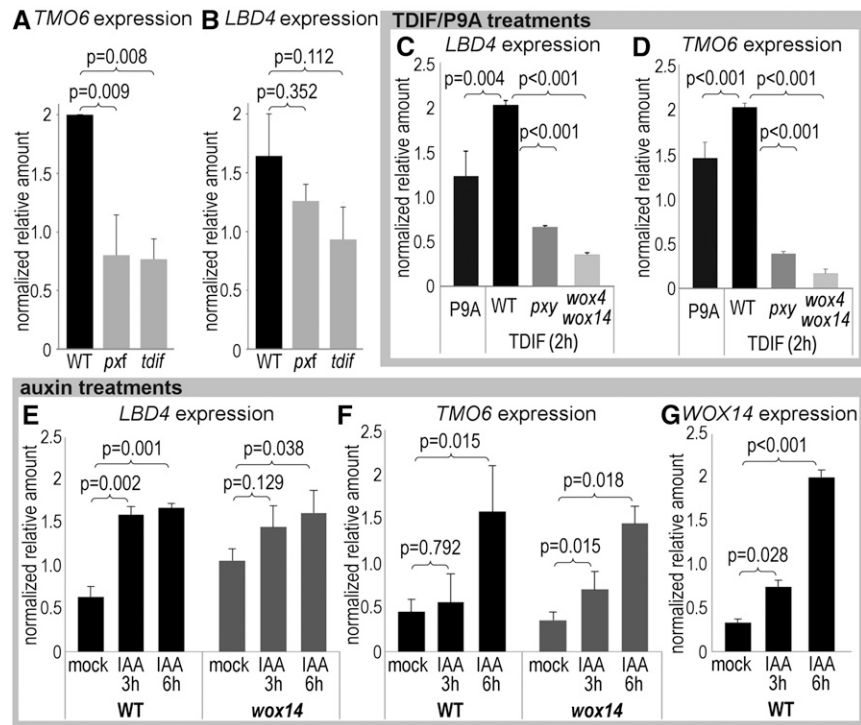


Figure 4. PXy and Auxin Signaling Regulate the Feedforward Loop.

(A) and **(B)** qRT-PCR showing *TMO6* **(A)** and *LBD4* **(B)** expression in *pxf* and *tdif* lines.

(C) and **(D)** *LBD4* **(C)** and *TMO6* **(D)** expression in seedlings treated with TDIF or P9A for 2 h.

(E) to **(G)** qRT-PCR showing *LBD4* **(E)**, *TMO6* **(F)**, and *WOX14* **(G)** expression in seedlings treated with IAA for 3 or 6 h.

Expression differences were determined in technical triplicate for each of three biological replicates. Tissue for each biological replicate was taken from a different plate. P values marked on critical comparisons were determined using ANOVA and an LSD posthoc test ($n = 3$ biological replicates; error bars are SE).

single mutant was similar to that of the wild-type controls (Figures 2F and 2G; Supplemental Figures 3A and 3B; Supplemental Data Set 5). To eliminate functional redundancy, we crossed *lbd4* to a T-DNA insertion line of *LBD3*, the gene most similar to *LBD4* (Shuai et al., 2002). A reduction in vascular cell number was observed in *lbd3 lbd4* double mutants (Supplemental Figures 3D and 3E).

LBD4 is expressed at the procambium-phloem boundary (Figure 3A). Thus, we determined phloem cell number in the *lbd3 lbd4* double mutants and controls, but no differences were observed (Supplemental Figure 3E; Supplemental Data Set 5). We also measured the distribution of phloem along the radial axis in these lines. The *lbd3 lbd4* double mutants had a thinner band of phloem in vascular bundles than the control lines (Supplemental Figure 3F), although this did not influence overall vascular bundle shape, as judged by measuring the tangential:radial ratio (Supplemental Figure 3G). Other members of the *LBD* gene family define boundaries at the edges of the apical meristem and the lateral root (Okushima et al., 2007; Bell et al., 2012). *LBD4* is expressed at the phloem-procambium boundary and influences phloem distribution redundantly with *LBD3*. Thus, we reasoned that *LBD4* might influence boundaries within vascular tissue. To explore this idea, we manipulated the *LBD4* expression domain. *LBD4* expression was

restored ectopically in companion cells of the phloem using a *SUC2:LBD4* construct or in the xylem using an *IRX3:LBD4* construct, both within the *lbd4* mutant background (Figure 5). In *lbd4 SUC2:LBD4* lines, an increase in the total number of cells per vascular bundle was observed. While xylem cell number did not differ between genotypes, both phloem and procambium cell numbers were higher in *lbd4 SUC2:LBD4* than in the other lines (Figure 5D).

We observed reduced secondary cell wall deposition in the fiber cells of *lbd4 IRX3:LBD4* lines (Figures 5A and 5C), indicating that xylem differentiation was disrupted, although the total number of cells in the xylem did not change (Figure 5D). In terms of overall vascular bundle shape within these different backgrounds, the ratio of the length of the tangential to the radial axes of vascular bundles was 0.65 in the wild type, which is similar to that observed in *lbd4* and *lbd4 SUC2:LBD4* lines (Figure 5E). By contrast, the ratio increased to 0.96 in *lbd4 IRX3:LBD4* vascular bundles, demonstrating a reduction in vascular expansion along the radial axis relative to the tangential axis. Furthermore, phloem distribution was dramatically different in the *LBD4* misexpression lines. The *lbd4 SUC2:LBD4* lines exhibited a wider band of phloem along the radial axis compared with the other lines tested (Figure 5E). While this can be explained in part by changes to phloem cell number, the

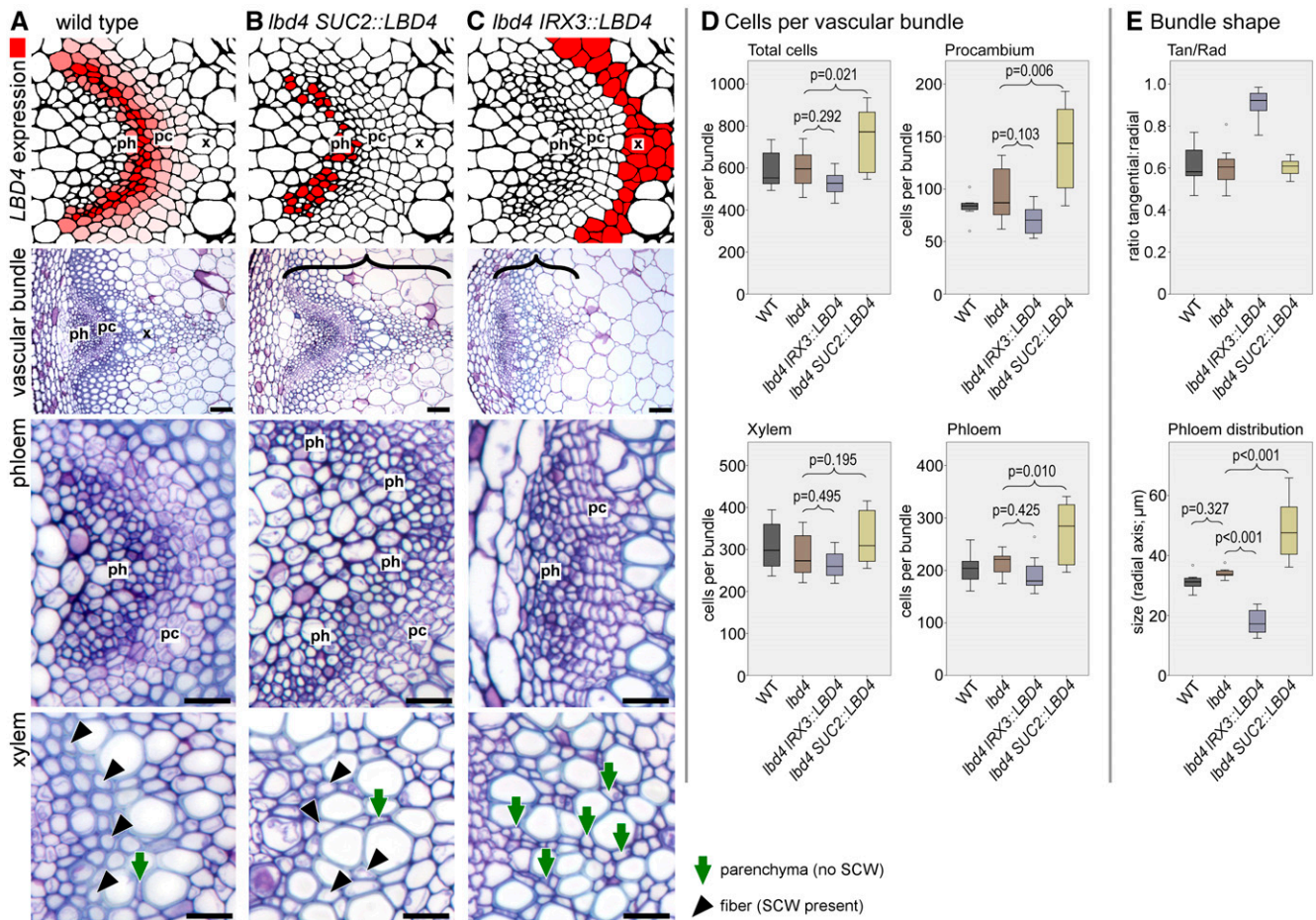


Figure 5. *LBD4* Expression Patterns the Vascular Tissue.

(A) to (C) Consequences of *LBD4* expression at the phloem-procambium boundary (A), in phloem (B), or in xylem (C) in inflorescence stems. Upper panels show diagrammatic representation of the *LBD4* expression domain, with subsequent panels showing overall vascular morphology, phloem (ph), and xylem (x). pc, cambium; SCW, secondary cell wall. The radial axis is marked in (B) and (C) with a black bracket. Bars = 50 μm (whole vascular bundle) and 20 μm (xylem and phloem closeups).

(A) Wild-type vascular bundle showing an arc of phloem cells, procambium cells, and xylem cells along the radial axis of a stem transverse section. Xylem is characterized by the presence of fiber cells with large secondary cell walls (black arrowheads).

(B) *lbd4 SUC2::LBD4* lines have an increased phloem size. Xylem fiber cells retain secondary cell walls (black arrowheads). Parenchyma, with no secondary cell wall, is marked with a green arrow.

(C) *lbd4 IRX3::LBD4* lines demonstrate a change to phloem morphology, as the characteristic arc is absent. Cells where fibers were observed in wild-type xylem do not have large secondary cell walls (parenchyma; green arrows).

(D) Boxplots showing the mean number of total cells per vascular bundle (upper left) and number of procambium (upper right), phloem (lower right), and xylem (lower left) cells per vascular bundle. P values were determined using ANOVA with an LSD posthoc test ($n = 7$).

(E) The upper boxplot shows vascular bundle shape determined by measuring the ratio of the tangential to the radial axis, and the lower boxplot shows the distribution of phloem along the radial axis of the stem. P values were determined using ANOVA with an LSD posthoc test ($n = 7$).

Boxplots show median (inner line) and inner quartiles (box). Whiskers extend to the highest and lowest values no greater than 1.5 times the inner quartile range, and circles show outliers.

same cannot be said of changes to phloem distribution in *lbd4 IRX3::LBD4* lines. Here, despite similar numbers of phloem cells relative to the wild type or *lbd4* single mutants (Figure 5D), these phloem cells were distributed in a much narrower band (Figure 5E). The redistribution of phloem cells accompanied by changes to vascular bundle shape could be caused by a failure to correctly mark the phloem-procambium boundary.

The Vascular Function of *LBD4* is *PXY/TDIF*-Dependent

pxy and *tdif* mutants demonstrate intercalation of vascular cell types (i.e., a loss of clearly defined boundaries; Figure 6; Supplemental Figure 6; Fisher and Turner, 2007; Etchells and Turner, 2010; Wang et al., 2018). These mutants are also characterized by reductions in vascular cell number (Hirakawa et al., 2008). To investigate genetic interactions between *pxy* and *lbd4*,

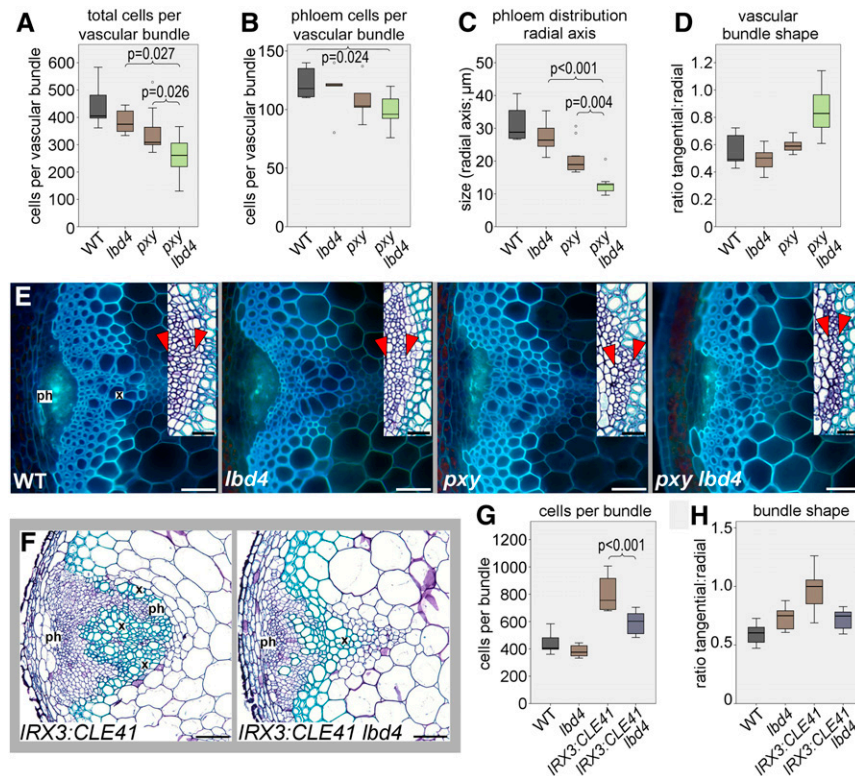


Figure 6. Genetic Interactions between *LBD4* and *TDIF-PXY*.

(A) to (E) Analysis of *pxy lbd4* double mutants and controls.

(A) and (B) Boxplots showing the total number of cells (A); $n = 7$) and the number of phloem cells (B); $n = 6$) per vascular bundle in 8-week-old inflorescence stems.

(C) Boxplot showing the distribution of phloem along the radial axis of the stem (distribution is shown on insets in E) as tissue between the red arrowheads; $n = 7$).

(D) Boxplot showing vascular bundle shape determined by measuring the ratio of the tangential to the radial axis ($n = 8$).

(E) Aniline blue-stained transverse sections of the wild type, *lbd4*, *pxy*, and *pxy lbd4*. Insets show closeups of phloem tissue stained with toluidine blue.

(F) to (H) *lbd4* suppresses *CLE41* misexpression phenotypes.

(F) *IRX3:CLE41* vascular bundles are characterized by organization defects, but these defects are attenuated in *IRX3:CLE41 lbd4* lines.

(G) and (H) Boxplots show the number of cells per vascular bundle (G) and vascular bundle shape determined by measuring the ratio of tangential to radial axis (H); $n = 6$).

Eight-week-old plants were used. Error bars are SE; P values in (A) to (C) and (G) were determined using ANOVA with an LSD posthoc test. ph, phloem; x, xylem. Boxplots show median (inner line) and inner quartiles (box). Whiskers extend to the highest and lowest values no greater than 1.5 times the inner quartile range, and circles show outliers. Bars = 50 μm , except for insets in (E), where bars = 20 μm .

we generated *pxy lbd4* double mutants. The gross morphology of these plants did not differ from that of the *pxy* single mutants, but *lbd4* enhanced the cell division phenotype of *pxy*, as *pxy lbd4* bundles had fewer cells per vascular bundle than the parental lines (Figure 6A; Supplemental Data Set 5). We counted the number of differentiated phloem cells to assess the recruitment of phloem precursors into the phloem. These numbers were similar in *pxy lbd4* lines compared with *pxy* and *lbd4* single mutants but were reduced compared with the wild type (Figure 6B; Supplemental Data Set 5). *lbd4* also enhanced the defect in phloem distribution along the vascular radial axis of *pxy* (Figure 6C and red arrowheads in Figure 6E). Finally, the tangential:radial axis ratio of vascular bundles was higher in the *lbd4 pxy* lines relative to the controls (Figure 6D), demonstrating a change to overall vascular bundle shape.

Vascular organization requires that *CLE41/42/44* generate a TDIF maximum in the phloem. Ectopic *CLE41* expression leads to intercalated xylem and phloem, presumably due to a change in the distribution of active TDIF-PXY complexes (Etchells and Turner, 2010). *LBD4* expression is elevated in response to TDIF-PXY (Figure 4C; Supplemental Table 1). Thus, we predicted that the defects of *IRX3:CLE41* would be attenuated in the absence of *LBD4*. Cell number within vascular bundles was unchanged in *lbd4* but significantly increased in *IRX3:CLE41* compared with the wild type (Figures 6F and 6G). Introduction of the *lbd4* mutation into *IRX3:CLE41* lines suppressed this phenotype. The tangential:radial ratio of *IRX3:CLE41 lbd4* lines was indistinguishable from that of the wild type and *lbd4* (Figure 6H). Thus, the changes to vascular bundle shape caused by the *IRX3:CLE41* construct were dependent on

LBD4. Intercalation of xylem and phloem was also reduced in *IRX3:CLE41 lbd4* compared with *IRX3:CLE41*. Finally, *lbd4* attenuated the gross morphological defects of *IRX3:CLE41* (Supplemental Figure 7). Thus, *lbd4* suppresses the *IRX3:CLE41* phenotype.

DISCUSSION

Integration of Transcriptional Regulators of Vascular Development

The study of vascular tissue development in plants has a long history. In addition to characterization by early plant anatomists, auxin in particular was found to influence vascular formation and connectivity in the 1950s and 1960s (Torrey, 1953; Sun, 1955; Sachs, 1969). In the 1990s, with the emergence of Arabidopsis as a genetic model, multiple genes were characterized as regulating vascular tissue formation (Lincoln et al., 1990; Berleth and Jurgens, 1993; Baima et al., 1995; Zhong et al., 1997; Gälweiler et al., 1998), and such discoveries have been accelerating in the postgenomic era (Ruonala et al., 2017; Fischer et al., 2019). Recently, those taking genetic, biochemical, and mathematical approaches to studying vascular development have elegantly described how a subset of these components interact (De Rybel et al., 2014; Kondo et al., 2014; Muraro et al., 2014; Vera-Sirera et al., 2015; Mellor et al., 2017; Han et al., 2018; Miyashima et al., 2019; Smet et al., 2019). Here, we used an eY1H approach to map a network with 312 nodes and 690 interactions that describes how numerous components may come together to control the patterning and proliferation of vascular tissue (Figure 1A). Because we screened the promoters of components involved in auxin perception, cytokinin perception, PXY receptors, ER receptors, and GSK3 kinases, the network can be used to identify transcription factors that integrate these signals. This set of transcription factor-promoter interactions represents PXY-mediated transcriptional regulation, as perturbations in the TDIF-PXY signaling pathway (genes differentially expressed in *pxy* mutants and in *35S:CLE41* lines) are significantly enriched within our network (Supplemental Figure 2).

The TMO6-WOX14-LBD4 Feedforward Loop Is Essential for Vascular Development

The power of our network as a resource for identifying novel interactions was demonstrated by characterizing the TMO6-WOX14-LBD4 feedforward loop. We investigated the nature of this regulatory circuit using eY1H, LUC reporter assays, qRT-PCR, and genetic interaction analysis. The regulatory circuit appears to be central to vascular cell proliferation, as evidenced by the loss of 41% of vascular bundle cells in *tmo6 wox14 lbd4* lines relative to the wild type (Figure 2F). We demonstrated that the feedforward loop is regulated by auxin and TDIF-PXY signaling (Figures 3F–3K, 4A–4D–4D, and 6; Supplemental Table 1; Etchells et al., 2013). Given that TMO6 has also been shown to be an integrator of cytokinin signaling (Schlereth et al., 2010; Miyashima et al., 2019;

Smet et al., 2019), this circuit likely acts as an integration point for many critical developmental regulators.

The transcription of *HD-Zip III* genes is thought to be activated by the TMO6 paralogue PEAR1 during primary patterning of the root vascular cylinder (Miyashima et al., 2019). In our eY1H assays, both PEAR1 and TMO6 bound to the promoters of the *HD-Zip III* genes *PHB*, *PHV*, and *REV* (Figure 1A; Supplemental Data Set 2). *HD-Zip III* expression is thought to represses *PEAR1* transcription in a negative feedback loop (Miyashima et al., 2019), and *PHV* bound the *TMO6* promoter in our eY1H assay (Figure 1A; Supplemental Data Set 2). Therefore, it would be interesting to further study interactions between *HD-Zip III* genes, *PEAR1*, and members of the feed-forward loop.

Members of the Feed-Forward Loop May Function Redundantly with Paralogues

Genetic redundancy, such as that uncovered by Miyashima et al. (2019), is a possible explanation for the finding that the *tmo6* mutants demonstrated no changes in *LBD4* expression (Figure 3F). Genetic redundancy might also explain the lack of mutant phenotypes for individual *LBD* family members. A recent genetic analysis aimed at characterizing regulators of the vascular cambium in Arabidopsis roots also identified *LBD4* as a putative vascular regulator (Zhang et al., 2019). *lbd1 lbd4* lines exhibited reduced vascular tissue area in roots. Since we demonstrated that *lbd4* acts redundantly with *lbd3* (Supplemental Figure 3), it is tempting to speculate that there may be genetic redundancy between these three paralogues.

Control of Vascular Bundle Size and Shape

TMO6, *WOX14*, and *LBD4* are jointly expressed at the phloem-procambium boundary in the vascular tissue of inflorescence stems (Figures 3A to 3C). These genes also act within a coherent type I feedforward loop (Mangan and Alon, 2003), as all are positive transcriptional activators. *WOX14* was sufficient to activate *TMO6* expression in wild tobacco protoplasts (Supplemental Figure 5) and was also required for normal expression of *TMO6* in Arabidopsis stems (Figure 3D). *WOX14* activated *LBD4* reporter expression in wild tobacco protoplasts when coexpressed with *TMO6* (Supplemental Figure 5A). Both *WOX14* and *TMO6* were required for the very highest levels of *LBD4* expression in wild tobacco (Supplemental Figure 5A). Such synergism may also explain why *tmo6* mutants alone did not demonstrate changes to *LBD4* expression but *pxf tmo6* (where *WOX14* expression is reduced) and *wox4 wox14 tmo6* lines did (Figure 3F).

WOX genes and their targets are crucial for regulating stem cell fate in plant meristems (Laux et al., 1996; Sarkar et al., 2007; Ji et al., 2010; Etchells et al., 2013), but the roles of direct *WOX* targets in the vascular stem cell niche have been unclear. Modeling of transcriptome data by Zhang et al. (2019) also placed *WOX14* upstream of *LBD4*. The data presented here provide additional support for this interaction (Figures 1B and 3D to 3F; Supplemental Figure 5).

Organ Boundaries Are Marked by Members of the LBD Family

Members of the *LBD/AS2* gene family (Iwakawa et al., 2002; Shuai et al., 2002) regulate the formation of organ boundaries during lateral root formation (Okushima et al., 2007) and at the shoot apex (Bell et al., 2012) in *Arabidopsis*. In hybrid poplar (*Populus tremula* × *Populus alba*), the overexpression of *PtaLBD1* increases secondary phloem production (Yordanov et al., 2010). Here, we determined that *LBD4* is expressed at the phloem-procambium boundary (Figure 3A). An increase in vascular bundle cell number was observed in *lbd4 SUC2:LBD4* lines, where *LBD4* expression was shifted to the phloem. Increases in cell number were restricted to the procambium and phloem. Strikingly, no change in the number of xylem cells was observed (Figure 5D). These data suggest that *LBD4* controls phloem cell recruitment in a spatially restricted manner (Figures 5A, 5B, and 5E). The loss of normal xylem differentiation in *lbd4 IRX3:LBD4* bundles where *LBD4* expression was shifted to the xylem (Figure 5C) suggests that this occurs in part by excluding xylem identity from the phloem side of the procambium. *LBD4* could mark the phloem-procambium boundary via regulation by TDIF-PXY, WOX14, and TMO6. Notably, *TMO6* and its paralogues are thought to define the zone of procambial activity in the root (Miyashima et al., 2019). The definition of the procambium domain could be considered to include marking its edges. Thus, *LBD4* could act as a boundary regulator or as an amplifier of divisions on the phloem side of the procambium. These putative functions are not necessarily mutually exclusive.

TDIF-PXY and LBD4

pxy mutants are characterized by intercalation of xylem and phloem (Fisher and Turner, 2007). For such phenotypes to occur, boundary specification must be disrupted. In *pxy lbd4* mutants, the positions of tissues were altered because phloem was distributed differently along the radial axis of the stem (Figure 6C) and bundle shape was altered (Figure 6D). *lbd4 pxy* plants also demonstrated reductions in vascular cell division (Figures 6A and 6B). PXY-regulated vascular organization is dependent on *CLE41* acting as a phloem-derived positional cue. Dramatic vascular reorganization occurs when *CLE41* is expressed from the xylem in *IRX3:CLE41* lines because the position of active TDIF-PXY complexes is altered (Etchells and Turner, 2010). In turn, this leads to changes in the positions of xylem, phloem, and procambium (Figure 6F), and as such, these tissues are found in ectopic positions relative to the wild type. Consequently, boundaries between the phloem and procambium must also be present in ectopic positions in *IRX3:CLE41*. Our observation that the *IRX3:CLE41* phenotype was strongly suppressed by *lbd4* supports the hypothesis that *LBD4* marks the phloem-procambium boundary, since in *lbd4 IRX3:CLE41* plants, phloem was restored to the position it occupied in the wild type (Figure 6F). Therefore, the putative ectopic *LBD4*-specified boundary tissue observed in *IRX3:CLE41* lines was removed in these plants.

In conclusion, a genetic interaction between *LBD4* and *PXY* regulates vascular bundle shape. *LBD4* also determines stem cell number in the vascular meristem via regulation by *TMO6* and

WOX14 and redundantly with *LBD3*. Our PXY-mediated transcriptional network provides a framework for exploring other interacting regulators at the transcriptional level.

METHODS

Gene Expression Analysis

Microarray analysis was used to compare the transcriptomes of *Arabidopsis thaliana* ecotype Columbia 0 (Col-0) and 35S:*CLE41*; the experimental setup, preparation of total RNA, synthesis of biotinylated cDNA, subsequent hybridization to ATH1 Affymetrix GeneChip oligonucleotide arrays, and detection were previously described by Etchells et al. (2012). Briefly, following germination on Murashige and Skoog (MS) agar plates, plants were transferred to soil and grown under long-day conditions (see below) for 5 weeks. Inflorescence stems were harvested, stripped of side branches, and divided into four sections of equal size. RNA was isolated from the third section from the top using TRIzol (Invitrogen). Samples were prepared in triplicate for each genotype, and following RNA extraction, processing was performed at the University of Manchester Genomic Technologies Facility (<http://www.ls.manchester.ac.uk/research/facilities/microarray/>). Technical quality control was performed as described by Li and Wong (2001), and background correction, normalization, and gene expression analysis were performed using RMA in Bioconductor (Bolstad et al., 2003). Differential expression analysis was performed using Limma (Smyth, 2004). No probe is present for the *WOX4* gene on this microarray chip.

Gene expression in inflorescence stems was compared by qRT-PCR using RNA isolated with TRIzol reagent (Life Technologies). Samples were measured in technical triplicates (reactions per sample) on biological triplicates (independent samples per genotype and/or treatment). The RNA was DNase treated with RQ1 (Promega) prior to cDNA synthesis using a poly-T primer and BioScript reverse transcriptase (Bioline). qPCR BIO SyGreen Mix (PCR Biosystems) and primers described in Supplemental Data Set 6 were used with a CFX Connect machine (Bio-Rad). Relative expression was determined using a comparative C_T method using average amplification efficiency for each primer pair, as determined using LinReg (Ramakers et al., 2003). Samples were normalized to 18S rRNA (not shown) and *ACT2* (shown). Results were similar regardless of the control used.

To characterize changes in gene expression in response to TDIF and P9A peptides, or IAA application, seeds were stratified prior to incubation in a Sanyo MLR-351H plant growth chamber set to 23°C and constant light on half strength MS medium with 1% (w/v) agar. At 5 d, seedlings were transferred to liquid half strength MS medium containing either 5 μM TDIF (His-Glu-Val-Hyp-Ser-Gly-Hyp-Asn-Pro-Ile-Ser-Asn) or negative control P9A (His-Glu-Val-Hyp-Ser-Gly-Hyp-Asn-Ala-Ile-Ser-Asn; Bachem), or 10 μM IAA. Plants were maintained on a rocking platform for 1 h, snap-frozen in liquid nitrogen, and subjected to RNA extraction and qRT-PCR analysis as described above.

eY1H Assays

Yeast (*Saccharomyces cerevisiae*) cells were grown using standard methods (Brady et al., 2011; Gaudinier et al., 2011; Reece-Hoyes et al., 2011; Taylor-Teeple et al., 2015). Briefly, YPDA medium was used for unrestrained growth. –Trp, –His–Ura, or –His–Ura–Trp (containing 3-aminotriazole [3AT] when necessary) medium was used to apply selection. The transcription factor library contained 812 unique cDNAs fused to the GAL4 activation domain in pDEST-AD-2μ, which are maintained as plasmids in yeast and enable growth on –Trp medium. For promoter clones, promoter fragments (1.2–3.5 kb) were amplified using LA taq (Takara) and cloned using 5' TOPO (Life Technologies). These entry clones were used to create reporter constructs via Gateway recombination. The use of pMW2

clones enabled selection on –His medium and detection of interactions via growth on plates supplemented with 3AT. pMW3 (selection on –Ura medium) contained a LacZ reporter. Both vectors were transformed into yeast strain YM4271, integrated into the yeast genome via homologous recombination, and selected on –His–Ura plates. Colonies with no autoactivation in X-Gal that grew on moderate 3AT concentrations (10–100 mM) were selected. The presence of both reporters was confirmed by PCR.

eY1H was performed as described (Gaudinier et al., 2011; Reece-Hoyes et al., 2011) using a ROTOR HDA robot (Singer). Briefly, mating was performed by combining yeast cells containing the transcription factor and promoter constructs on a YPDA plate. After diploid selection using –His–Ura–Trp plates, the diploids were plated onto plates supplemented with 3AT and onto YPDA plates containing a nitrocellulose filter. Following 2 d of growth at room temperature, the nitrocellulose filters were subjected to an X-Gal assay. For 3AT plates, the plates were checked daily for colonies with increased growth. A network was subsequently constructed by importing the directional interactions into Cytoscape.

Testing Transcription Factor-Promoter Interactions

To test transcription factor-promoter interactions using a dual luciferase assay system, target promoters were cloned upstream of the *LUC* reporter gene in pGreenII-0800-LUC, which also contained a *35S:REN* control cassette. Transcription factor sequences were cloned behind the *35S* promoter in pGreenII 62-SK (Hellens et al., 2005). A ClonExpress II One Step Cloning Kit (Vazyme) and primers listed in Supplemental Data Set 6 were used for vector construction. Reporter detection was performed using the Dual-Luciferase Reporter Assay System (Promega). Boxplots in Supplemental Figure 5 show data from four biological replicates.

Wild tobacco (*Nicotiana benthamiana*) leaf protoplasts were generated by immersing leaf material in a solution containing 1.5% (w/v) Cellulase R10 (Yakult), 0.2 to 0.4% (w/v) Macerozyme R10 (Yakult), 1% (w/v) Hemicellulase (Sigma-Aldrich), 0.4 M mannitol, 20 mM KCl, 20 mM MES (pH 5.7), 10 mM CaCl₂, and 0.1% (w/v) BSA for 12 h. An equal volume of W5 solution (150 mM NaCl, 125 mM CaCl₂, 5 mM KCl, and 2 mM MES [pH 5.7]) was added prior to passing the mixture through a 200-mesh sieve. Protoplasts were collected by centrifugation and resuspended in ice-cold W5 (Duarte et al., 2016). Purified plasmids were transferred into these cells using the polyethylene glycol-calcium method with minor modifications (Yoo et al., 2007).

Generation of Plant Stocks

Seeds were stratified for 2 d at 4°C in 0.1% (w/v) agar prior to sowing on F2 compost (Levington) or on MS medium and 1% (w/v) agar on vertical plates. Plants were grown at 22°C under long-day conditions (16 h of light/8 h of dark, 300 μmol m⁻² s⁻¹, provided by cool-white fluorescent bulbs, supplemented with incandescent lighting).

Seed lines were all in the Col-0 background. *35S:CLE41*, *pxy-3*, *wox4*, *wox14*, *IRX3:CLE41*, *IRX3:CLE41 wox4*, and *pxf (pxy pxl1 pxl2)* have been described previously by Fisher and Turner (2007), Etchells and Turner (2010), Hirakawa et al. (2010), and Etchells et al. (2013; Supplemental Table 4). *lbd3* (WiscDsLoxHs070_10G; Woody et al., 2007) and *lbd4* (Salk_146141; Alonso et al., 2003) mutant lines (Supplemental Table 4) were identified using the TAIR database (Swarbreck et al., 2008) and confirmed using PCR. The *lbd4* allele harbored the T-DNA insertion in the *LBD4* 5' untranslated region, and we could not detect *LBD4* mRNA using qRT-PCR. *pxylbd4*, *lbd3lbd4*, *wox4lbd4*, and *IRX3:CLE41lbd4* lines were identified in segregating F2 populations by PCR. *tmo6* lines (Supplemental Table 4) were generated by genome editing (Xing et al., 2014; Wang et al., 2015). Target sequences AAGAAACCTTCTCCTGCAA and CTCTAAGGAACA TCCCCGTG were identified using clustered regularly interspaced short palindromic repeats (CRISPR)-PLANT (Xie et al., 2014) and tested for off-

targets (Bae et al., 2014). Primers incorporating the target sequences (Supplemental Data Set 6) were used in a PCR with plasmid pCBC-DT1T2 as template to generate a PCR product with a *TMO6* guide RNA, which was in turn incorporated into pHEE2E-TRI using a Golden Gate reaction. The resulting *TMO6* CRISPR/Cas9 clone was transferred to Arabidopsis by the floral dip method (Clough and Bent, 1998). Mutants were selected with primers that flanked the guide RNA target sites (Supplemental Figure 8). Oligonucleotides used for genotyping are described in Supplemental Data Set 6.

The CRISPR construct used to generate the *tdif (cle41,42,43,44)* mutant was built using the *pCUT* vector system (Peterson et al., 2016). For each of the four targeted CLE genes, a 20-bp guide RNA (gRNA) target site was selected upstream of the dodecapeptide coding region in the genomic sequence. A gRNA gene array was synthesized by GeneArt (Thermo Fisher Scientific) as a group of four *AtU6:gRNA* tandem constructs, which was subsequently cloned into the *pCUT4* binary vector via restriction enzyme digestion methods as previously described by Peterson et al. (2016). Col-0 plants were transformed with the CRISPR binary construct via the floral dip method, and T1 transgenic seed derived was selected on B5 medium without sucrose and containing 100 mg/L hygromycin. The T1 generation was screened for editing efficiency by sequencing the CLE gene PCR products amplified from leaf DNA. Plants confirmed to have efficient editing had overlapping sequence traces originating at the –3 position from the protospacer adjacent motif. T2 seed derived from plants with efficient editing was grown on selective B5 medium, DNA was collected, and each of the four CLE target genes was amplified via PCR. The products were sequenced directly via Sanger sequencing using primers listed in Supplemental Data Set 6. These plants demonstrated a *pxy*-like phenotype, which was partially recoverable by transformation with a *SUC2:CLE41* construct (Supplemental Figure 6) that was described previously (Etchells and Turner, 2010).

The *wox14 lbd4 tmo6* lines and respective double mutants were identified in F2 and F3 populations. *IRX3:LBD4* and *SUC2:LBD4* lines were generated by PCR amplification of a genomic fragment incorporating the *LBD4* coding region, which was cloned into pENTR-D-TOPO prior to transfer into plasmid p3KC (Atanassov et al., 2009). For *SUC2:LBD4*, the *IRX3* promoter in p3KC was replaced with that of *SUC2*. The resulting overexpression clone was introduced into Arabidopsis using the floral dip method (Clough and Bent, 1998).

Histology

Plant vascular tissue visualization was performed in 4-μm resin sections stained with 0.05% (w/v) aqueous toluidine blue, following fixation of plant material in formaldehyde - acetic acid - alcohol, dehydration through an ethanol series, and embedding in JB4 resin. Alternatively, hand sections were stained with 500 mM aniline blue dissolved in 100 mM phosphate buffer, pH 7.2, and viewed under a UV light lamp.

Accession Numbers

The accession numbers of the factors central to this article are CLE41 (AT3G24770), CLE42 (AT2G34925), CLE44 (AT4G13195), LBD3 (AT1G16530), LBD4 (AT1G31320), PXL1 (AT1G08590), PXL2 (AT4G28650), PXY (AT5G61480), TMO6 (AT5G60200), WOX4 (AT1G46480), and WOX14 (AT1G20700). For a comprehensive list of accession numbers represented in the eY1H data, please see Supplemental Data Set 2. Microarray data have been submitted in a MIAME compliant standard to the Gene Expression Omnibus (accession number GSE123162).

Supplemental Data

Supplemental Figure 1. qRT-PCR confirmation of microarray experiment.

Supplemental Figure 2. Network of genes misexpressed in different genetic backgrounds.

Supplemental Figure 3. Vascular tissue in *lbd3 lbd4* double mutants.

Supplemental Figure 4. In situ controls, and *LBD4* expression along the apical-basal axis of wild type and *pxy* mutant stems

Supplemental Figure 5. *LBD4pro:LUC* expression in the presence of WOX14 and TMO6.

Supplemental Figure 6. Phenotype of *cle41 cle42 cle43 cle44* quadruple mutants.

Supplemental Figure 7. *lbd4* suppresses the *IRX3:CLE41* phenotype.

Supplemental Figure 8. Genome edited *tmo6* allele.

Supplemental Table 1. Expression of genes demonstrating expression changes in 35S:*CLE41* compared with wild type in array data analyzed in this study.

Supplemental Table 2. Promoters analyzed using Y1H.

Supplemental Table 3. P-values for qRT-PCR analysis of *LBD4* expression differences in *pxf tmo6* and *wox4 wox14 tmo6* mutants and controls.

Supplemental Table 4. Plant lines used in this manuscript.

Supplemental Data Set 1. Differentially expressed genes in 35S:*CLE41* compared with wild type, as determined using microarrays.

Supplemental Data Set 2. Transcription factor-promoter interactions identified in eY1H.

Supplemental Data Set 3. List of interacting transcription factors and the transcription factors families that they represent.

Supplemental Data Set 4. Promoters arranged in order of those with the most to fewest interacting transcription factors.

Supplemental Data Set 5. Pairwise P-values for all comparisons of vascular phenotypes in this article.

Supplemental Data Set 6. Oligonucleotides used in this study.

ACKNOWLEDGMENTS

We thank Dória de Souza Etchells for technical assistance. This work was supported by the European Commission (Marie Skłodowska-Curie fellowship 329978-Vascular gene maps to J.P.E), N8 Agrifood (pump priming funds to J.P.E. and S.R.T.), the Jo Kolk Study Fund from the VVAO (to M.E.S.), the National Science Foundation Plant Genome Research Program (IOS-1546837 to Z.L.N.), and the Howard Hughes Medical Institute (Faculty Scholar Fellowship to S.M.B.).

AUTHOR CONTRIBUTIONS

S.M.B., J.P.E., S.R.T., D.W., J.T.K., X.Y., H.S., and Z.L.N. designed the experiments; M.E.S., S.M., H.S., C.G., A.-M.B., C.L.S., A.G., C.J.W., J.T.K., and J.P.E. performed the experiments; all authors analyzed the data; J.P.E. and S.M.B. drafted the article.

Received July 29, 2019; revised November 12, 2019; accepted December 5, 2019; published December 5, 2019.

REFERENCES

- Alonso, J.M., et al. (2003). Genome-wide insertional mutagenesis of *Arabidopsis thaliana*. *Science* **301**: 653–657.
- Atanassov, I.I., Atanassov, I.I., Etchells, J.P., and Turner, S.R. (2009). A simple, flexible and efficient PCR-fusion/Gateway cloning procedure for gene fusion, site-directed mutagenesis, short sequence insertion and domain deletions and swaps. *Plant Methods* **5**: 14.
- Bae, S., Park, J., and Kim, J.-S. (2014). Cas-OFFinder: A fast and versatile algorithm that searches for potential off-target sites of Cas9 RNA-guided endonucleases. *Bioinformatics* **30**: 1473–1475.
- Baima, S., Forte, V., Possenti, M., Peñalosa, A., Leoni, G., Salvi, S., Felici, B., Ruberti, I., and Morelli, G. (2014). Negative feedback regulation of auxin signaling by ATHB8/ACL5-BUD2 transcription module. *Mol. Plant* **7**: 1006–1025.
- Baima, S., Nobili, F., Sessa, G., Lucchetti, S., Ruberti, I., and Morelli, G. (1995). The expression of the Athb-8 homeobox gene is restricted to provascular cells in *Arabidopsis thaliana*. *Development* **121**: 4171–4182.
- Baima, S., Possenti, M., Matteucci, A., Wisman, E., Altamura, M.M., Ruberti, I., and Morelli, G. (2001). The *Arabidopsis* ATHB-8 HD-zip protein acts as a differentiation-promoting transcription factor of the vascular meristems. *Plant Physiol.* **126**: 643–655.
- Bell, E.M., Lin, W.C., Husbands, A.Y., Yu, L., Jaganatha, V., Jablonska, B., Mangeon, A., Neff, M.M., Girke, T., and Springer, P.S. (2012). *Arabidopsis* lateral organ boundaries negatively regulates brassinosteroid accumulation to limit growth in organ boundaries. *Proc. Natl. Acad. Sci. USA* **109**: 21146–21151.
- Berleth, T., and Jurgens, G. (1993). The role of the *monopteros* gene in organising the basal body region of the *Arabidopsis* embryo. *Development* **118**: 575–587.
- Bolstad, B.M., Irizarry, R.A., Astrand, M., and Speed, T.P. (2003). A comparison of normalization methods for high density oligonucleotide array data based on variance and bias. *Bioinformatics* **19**: 185–193.
- Brackmann, K., et al. (2018). Spatial specificity of auxin responses coordinates wood formation. *Nat. Commun.* **9**: 875.
- Brady, S.M., et al. (2011). A stele-enriched gene regulatory network in the *Arabidopsis* root. *Mol. Syst. Biol.* **7**: 459.
- Caño-Delgado, A., Yin, Y., Yu, C., Vafeados, D., Mora-García, S., Cheng, J.C., Nam, K.H., Li, J., and Chory, J. (2004). BRL1 and BRL3 are novel brassinosteroid receptors that function in vascular differentiation in *Arabidopsis*. *Development* **131**: 5341–5351.
- Carlsbecker, A., et al. (2010). Cell signalling by microRNA165/6 directs gene dose-dependent root cell fate. *Nature* **465**: 316–321.
- Chen, M.-K., Wilson, R.L., Palme, K., Ditengou, F.A., and Shpak, E.D. (2013). ERECTA family genes regulate auxin transport in the shoot apical meristem and forming leaf primordia. *Plant Physiol.* **162**: 1978–1991.
- Cho, H., et al. (2014). A secreted peptide acts on BIN2-mediated phosphorylation of ARFs to potentiate auxin response during lateral root development. *Nat. Cell Biol.* **16**: 66–76.
- Clough, S.J., and Bent, A.F. (1998). Floral dip: A simplified method for *Agrobacterium*-mediated transformation of *Arabidopsis thaliana*. *Plant J.* **16**: 735–743.
- De Rybel, B., et al. (2014). Plant development: Integration of growth and patterning during vascular tissue formation in *Arabidopsis*. *Science* **345**: 1255215.

- De Rybel, B., Möller, B., Yoshida, S., Grabowicz, I., Barbier de Reuille, P., Boeren, S., Smith, R.S., Borst, J.W., and Weijers, D. (2013). A bHLH complex controls embryonic vascular tissue establishment and indeterminate growth in Arabidopsis. *Dev. Cell* **24**: 426–437.
- Duarte, P., Ribeiro, D., Carqueijeiro, I., Bettencourt, S., and Sottomayor, M. (2016). Protoplast transformation as a plant-transferable transient expression system. In *Biotechnology of Plant Secondary Metabolism: Methods and Protocols*, A.G. Fett-Neto, ed (New York: Springer), pp. 137–148.
- Emery, J.F., Floyd, S.K., Alvarez, J., Eshed, Y., Hawker, N.P., Izhaki, A., Baum, S.F., and Bowman, J.L. (2003). Radial patterning of Arabidopsis shoots by class III HD-ZIP and KANADI genes. *Curr. Biol.* **13**: 1768–1774.
- Etchells, J.P., Provost, C.M., Mishra, L., and Turner, S.R. (2013). *WOX4* and *WOX14* act downstream of the PXY receptor kinase to regulate plant vascular proliferation independently of any role in vascular organisation. *Development* **140**: 2224–2234.
- Etchells, J.P., Provost, C.M., and Turner, S.R. (2012). Plant vascular cell division is maintained by an interaction between PXY and ethylene signalling. *PLoS Genet.* **8**: e1002997.
- Etchells, J.P., and Turner, S.R. (2010). The PXY-CLE41 receptor ligand pair defines a multifunctional pathway that controls the rate and orientation of vascular cell division. *Development* **137**: 767–774.
- Fischer, U., Kucukoglu, M., Helariutta, Y., and Bhalerao, R.P. (2019). The dynamics of cambial stem cell activity. *Annu. Rev. Plant Biol.* **70**: 293–319.
- Fisher, K., and Turner, S. (2007). PXY, a receptor-like kinase essential for maintaining polarity during plant vascular-tissue development. *Curr. Biol.* **17**: 1061–1066.
- Gälweiler, L., Guan, C., Müller, A., Wisman, E., Mendgen, K., Yephremov, A., and Palme, K. (1998). Regulation of polar auxin transport by AtPIN1 in Arabidopsis vascular tissue. *Science* **282**: 2226–2230.
- Gaudinier, A., Tang, M., Bågman, A.M., and Brady, S.M. (2017). Identification of protein-DNA interactions using enhanced yeast one-hybrid assays and a semiautomated approach. *Methods Mol. Biol.* **1610**: 187–215.
- Gaudinier, A., et al. (2011). Enhanced Y1H assays for Arabidopsis. *Nat. Methods* **8**: 1053–1055.
- Guo, Y., Qin, G., Gu, H., and Qu, L.-J. (2009). Dof5.6/HCA2, a Dof transcription factor gene, regulates interfascicular cambium formation and vascular tissue development in Arabidopsis. *Plant Cell* **21**: 3518–3534.
- Han, S., Cho, H., Noh, J., Qi, J., Jung, H.-J., Nam, H., Lee, S., Hwang, D., Greb, T., and Hwang, I. (2018). BIL1-mediated MP phosphorylation integrates PXY and cytokinin signalling in secondary growth. *Nat. Plants* **4**: 605–614.
- Hardtke, C.S., and Berleth, T. (1998). The Arabidopsis gene MONOPTEROS encodes a transcription factor mediating embryo axis formation and vascular development. *EMBO J.* **17**: 1405–1411.
- He, J.-X., Gendron, J.M., Yang, Y., Li, J., and Wang, Z.-Y. (2002). The GSK3-like kinase BIN2 phosphorylates and destabilizes BZR1, a positive regulator of the brassinosteroid signaling pathway in Arabidopsis. *Proc. Natl. Acad. Sci. USA* **99**: 10185–10190.
- Hellens, R.P., Allan, A.C., Friel, E.N., Bolitho, K., Grafton, K., Templeton, M.D., Karunairetnam, S., Gleave, A.P., and Laing, W.A.J.P.M. (2005). Transient expression vectors for functional genomics, quantification of promoter activity and RNA silencing in plants. *Plant Methods* **1**: 13.
- Hirakawa, Y., Kondo, Y., and Fukuda, H. (2010). TDIF peptide signaling regulates vascular stem cell proliferation via the *WOX4* homeobox gene in Arabidopsis. *Plant Cell* **22**: 2618–2629.
- Hirakawa, Y., Shinohara, H., Kondo, Y., Inoue, A., Nakanomyo, I., Ogawa, M., Sawa, S., Ohashi-Ito, K., Matsubayashi, Y., and Fukuda, H. (2008). Non-cell-autonomous control of vascular stem cell fate by a CLE peptide/receptor system. *Proc. Natl. Acad. Sci. USA* **105**: 15208–15213.
- Ikematsu, S., Tasaka, M., Torii, K.U., and Uchida, N. (2017). ERECTA-family receptor kinase genes redundantly prevent premature progression of secondary growth in the Arabidopsis hypocotyl. *New Phytol.* **213**: 1697–1709.
- Ito, Y., Nakanomyo, I., Motose, H., Iwamoto, K., Sawa, S., Dohmae, N., and Fukuda, H. (2006). Dodeca-CLE peptides as suppressors of plant stem cell differentiation. *Science* **313**: 842–845.
- Iwakawa, H., Ueno, Y., Semiarti, E., Onouchi, H., Kojima, S., Tsukaya, H., Hasebe, M., Soma, T., Ikezaki, M., Machida, C., and Machida, Y. (2002). The ASYMMETRIC LEAVES2 gene of Arabidopsis thaliana, required for formation of a symmetric flat leaf lamina, encodes a member of a novel family of proteins characterized by cysteine repeats and a leucine zipper. *Plant Cell Physiol.* **43**: 467–478.
- Ji, J., Strable, J., Shimizu, R., Koenig, D., Sinha, N., and Scanlon, M.J. (2010). *WOX4* promotes procambial development. *Plant Physiol.* **152**: 1346–1356.
- Kalir, S., Mangan, S., and Alon, U. (2005). A coherent feed-forward loop with a SUM input function prolongs flagella expression in *Escherichia coli*. *Mol. Syst. Biol.* **1**: 2005.0006.
- Kaplan, S., Bren, A., Dekel, E., and Alon, U. (2008). The incoherent feed-forward loop can generate non-monotonic input functions for genes. *Mol. Syst. Biol.* **4**: 203.
- Kim, T.-W., Michniewicz, M., Bergmann, D.C., and Wang, Z.-Y. (2012). Brassinosteroid regulates stomatal development by GSK3-mediated inhibition of a MAPK pathway. *Nature* **482**: 419–422.
- Kondo, Y., Ito, T., Nakagami, H., Hirakawa, Y., Saito, M., Tamaki, T., Shirasu, K., and Fukuda, H. (2014). Plant GSK3 proteins regulate xylem cell differentiation downstream of TDIF-TDR signalling. *Nat. Commun.* **5**: 3504.
- Konishi, M., Donner, T.J., Scarpella, E., and Yanagisawa, S. (2015). MONOPTEROS directly activates the auxin-inducible promoter of the Dof5.8 transcription factor gene in Arabidopsis thaliana leaf provascular cells. *J. Exp. Bot.* **66**: 283–291.
- Laux, T., Mayer, K.F., Berger, J., and Jürgens, G. (1996). The WUSCHEL gene is required for shoot and floral meristem integrity in Arabidopsis. *Development* **122**: 87–96.
- Le Hir, R., and Bellini, C. (2013). The plant-specific dof transcription factors family: New players involved in vascular system development and functioning in Arabidopsis. *Front. Plant Sci.* **4**: 164.
- Li, C., and Wong, W.H. (2001). Model-based analysis of oligonucleotide arrays: Expression index computation and outlier detection. *Proc. Natl. Acad. Sci. USA* **98**: 31–36.
- Lincoln, C., Britton, J.H., and Estelle, M. (1990). Growth and development of the *axr1* mutants of Arabidopsis. *Plant Cell* **2**: 1071–1080.
- Mangan, S., and Alon, U. (2003). Structure and function of the feed-forward loop network motif. *Proc. Natl. Acad. Sci. USA* **100**: 11980–11985.
- Mattsson, J., Ckurshumova, W., and Berleth, T. (2003). Auxin signaling in Arabidopsis leaf vascular development. *Plant Physiol.* **131**: 1327–1339.
- McConnell, J.R., Emery, J., Eshed, Y., Bao, N., Bowman, J., and Barton, M.K. (2001). Role of *PHABULOSA* and *PHAVOLUTA* in determining radial patterning in shoots. *Nature* **411**: 709–713.
- Mellor, N., Adibi, M., El-Showk, S., De Rybel, B., King, J., Mähönen, A.P., Weijers, D., and Bishopp, A. (2017). Theoretical approaches to understanding root vascular patterning: A consensus between recent models. *J. Exp. Bot.* **68**: 5–16.

- Miyashima, S., et al. (2019). Mobile PEAR transcription factors integrate positional cues to prime cambial growth. *Nature* **565**: 490–494.
- Morita, J., Kato, K., Nakane, T., Kondo, Y., Fukuda, H., Nishimasu, H., Ishitani, R., and Nureki, O. (2016). Crystal structure of the plant receptor-like kinase TDR in complex with the TDIF peptide. *Nat. Commun.* **7**: 12383.
- Müller, C.J., Valdés, A.E., Wang, G., Ramachandran, P., Beste, L., Uddenberg, D., and Carlsbecker, A. (2016). PHABULOSA mediates an auxin signaling loop to regulate vascular patterning in *Arabidopsis*. *Plant Physiol.* **170**: 956–970.
- Muraro, D., et al. (2014). Integration of hormonal signaling networks and mobile microRNAs is required for vascular patterning in *Arabidopsis* roots. *Proc. Natl. Acad. Sci. USA* **111**: 857–862.
- Ohashi-Ito, K., and Bergmann, D.C. (2007). Regulation of the *Arabidopsis* root vascular initial population by LONESOME HIGHWAY. *Development* **134**: 2959–2968.
- Ohashi-Ito, K., Saegusa, M., Iwamoto, K., Oda, Y., Katayama, H., Kojima, M., Sakakibara, H., and Fukuda, H. (2014). A bHLH complex activates vascular cell division via cytokinin action in root apical meristem. *Curr. Biol.* **24**: 2053–2058.
- Okushima, Y., Fukaki, H., Onoda, M., Theologis, A., and Tasaka, M. (2007). ARF7 and ARF19 regulate lateral root formation via direct activation of LBD/ASL genes in *Arabidopsis*. *Plant Cell* **19**: 118–130.
- Peterson, B.A., Haak, D.C., Nishimura, M.T., Teixeira, P.J.P.L., James, S.R., Dangi, J.L., and Nimchuk, Z.L. (2016). Genome-wide assessment of efficiency and specificity in CRISPR/Cas9 mediated multiple site targeting in *Arabidopsis*. *PLoS One* **11**: e0162169.
- Prigge, M.J., Otsuga, D., Alonso, J.M., Ecker, J.R., Drews, G.N., and Clark, S.E. (2005). Class III homeodomain-leucine zipper gene family members have overlapping, antagonistic, and distinct roles in *Arabidopsis* development. *Plant Cell* **17**: 61–76.
- Ragni, L., Nieminen, K., Pacheco-Villalobos, D., Sibout, R., Schwechheimer, C., and Hardtke, C.S. (2011). Mobile gibberellin directly stimulates *Arabidopsis* hypocotyl xylem expansion. *Plant Cell* **23**: 1322–1336.
- Ramachandran, P., Carlsbecker, A., and Etchells, J.P. (2016). Class III HD-ZIPs govern vascular cell fate: An HD view on patterning and differentiation. *J. Exp. Bot.* **68**: 55–69.
- Ramakers, C., Ruijter, J.M., Deprez, R.H.L., and Moorman, A.F.M. (2003). Assumption-free analysis of quantitative real-time polymerase chain reaction (PCR) data. *Neurosci. Lett.* **339**: 62–66.
- Reece-Hoyes, J.S., Diallo, A., Lajoie, B., Kent, A., Shrestha, S., Kadreppa, S., Pesyna, C., Dekker, J., Myers, C.L., and Walhout, A.J.M. (2011). Enhanced yeast one-hybrid assays for high-throughput gene-centered regulatory network mapping. *Nat. Methods* **8**: 1059–1064.
- Ruonala, R., Ko, D., and Helariutta, Y. (2017). Genetic networks in plant vascular development. *Annu. Rev. Genet.* **51**: 335–359.
- Sachs, T. (1969). Polarity and the induction of organized vascular tissues. *Ann. Bot. (Lond.)* **33**: 263–275.
- Sarkar, A.K., Luijten, M., Miyashima, S., Lenhard, M., Hashimoto, T., Nakajima, K., Scheres, B., Heidstra, R., and Laux, T. (2007). Conserved factors regulate signalling in *Arabidopsis thaliana* shoot and root stem cell organizers. *Nature* **446**: 811–814.
- Schlereth, A., Möller, B., Liu, W., Kientz, M., Flipse, J., Rademacher, E.H., Schmid, M., Jürgens, G., and Weijers, D. (2010). MONOPTEROS controls embryonic root initiation by regulating a mobile transcription factor. *Nature* **464**: 913–916.
- Shannon, P., Markiel, A., Ozier, O., Baliga, N.S., Wang, J.T., Ramage, D., Amin, N., Schwikowski, B., and Ideker, T. (2003). Cytoscape: A software environment for integrated models of biomolecular interaction networks. *Genome Res.* **13**: 2498–2504.
- Shen-Orr, S.S., Milo, R., Mangan, S., and Alon, U. (2002). Network motifs in the transcriptional regulation network of *Escherichia coli*. *Nat. Genet.* **31**: 64–68.
- Shuai, B., Reynaga-Peña, C.G., and Springer, P.S. (2002). The lateral organ boundaries gene defines a novel, plant-specific gene family. *Plant Physiol.* **129**: 747–761.
- Smet, W., et al. (2019). DOF2.1 controls cytokinin-dependent vascular cell proliferation downstream of TMO5/LHW. *Curr. Biol.* **29**: 520–529.e6.
- Smetana, O., et al. (2019). High levels of auxin signalling define the stem-cell organizer of the vascular cambium. *Nature* **565**: 485–489.
- Smyth, G.K. (2004). Linear models and empirical Bayes methods for assessing differential expression in microarray experiments. *Stat. Appl. Genet. Mol. Biol.* **3**: e3.
- Suer, S., Agusti, J., Sanchez, P., Schwarz, M., and Greb, T. (2011). WOX4 imparts auxin responsiveness to cambium cells in *Arabidopsis*. *Plant Cell* **23**: 3247–3259.
- Sun, C.N. (1955). Anomalous structure in the hypocotyl of soybean following treatment with 2,4-dichlorophenoxyacetic acid. *Science* **121**: 641.
- Swarbreck, D., et al. (2008). The *Arabidopsis* Information Resource (TAIR): Gene structure and function annotation. *Nucleic Acids Res.* **36**: D1009–D1014.
- Taylor-Teeples, M., et al. (2015). An *Arabidopsis* gene regulatory network for secondary cell wall synthesis. *Nature* **517**: 571–575.
- Torrey, J.G. (1953). The effect of certain metabolic inhibitors on vascular tissue differentiation in isolated pea roots. *Am. J. Bot.* **40**: 525–533.
- Uchida, N., Lee, J.S., Horst, R.J., Lai, H.-H., Kajita, R., Kakimoto, T., Tasaka, M., and Torii, K.U. (2012). Regulation of inflorescence architecture by intertissue layer ligand-receptor communication between endodermis and phloem. *Proc. Natl. Acad. Sci. USA* **109**: 6337–6342.
- Uchida, N., and Tasaka, M. (2013). Regulation of plant vascular stem cells by endodermis-derived EPFL-family peptide hormones and phloem-expressed ERECTA-family receptor kinases. *J. Exp. Bot.* **64**: 5335–5343.
- Vera-Sirera, F., De Rybel, B., Úrbez, C., Kouklas, E., Pesquera, M., Álvarez-Mahecha, J.C., Minguet, E.G., Tuominen, H., Carbonell, J., Borst, J.W., Weijers, D., and Blázquez, M.A. (2015). A bHLH-based feedback loop restricts vascular cell proliferation in plants. *Dev. Cell* **35**: 432–443.
- Waki, T., Miyashima, S., Nakanishi, M., Ikeda, Y., Hashimoto, T., and Nakajima, K. (2013). A GAL4-based targeted activation tagging system in *Arabidopsis thaliana*. *Plant J.* **73**: 357–367.
- Wang, N., Bagdassarian, K.S., Doherty, R.E., Kroon, J.T., Connor, K.A., Wang, X.Y., Wang, W., Jermyn, I.H., Turner, S.R., and Etchells, J.P. (2019). Organ-specific genetic interactions between paralogues of the PXY and ER receptor kinases enforce radial patterning in *Arabidopsis* vascular tissue. *Development* **146**: dev177105.
- Wang, N., Bagdassarian, K.S., Doherty, R.E., Wang, X.Y., Kroon, J.T., Wang, W., Jermyn, I.H., Turner, S.R., and Etchells, P. (2018). Paralogues of the PXY and ER receptor kinases enforce radial patterning in plant vascular tissue. *bioRxiv*. Available at: <https://doi.org/10.1101/357244>.
- Wang, Z.-P., Xing, H.-L., Dong, L., Zhang, H.-Y., Han, C.-Y., Wang, X.-C., and Chen, Q.-J. (2015). Egg cell-specific promoter-controlled CRISPR/Cas9 efficiently generates homozygous mutants for multiple target genes in *Arabidopsis* in a single generation. *Genome Biol.* **16**: 144.
- Woodward, C., Bemis, S.M., Hill, E.J., Sawa, S., Koshiba, T., and Torii, K.U. (2005). Interaction of auxin and ERECTA in elaborating

- Arabidopsis inflorescence architecture revealed by the activation tagging of a new member of the YUCCA family putative flavin monooxygenases. *Plant Physiol.* **139**: 192–203.
- Woody, S.T., Austin-Phillips, S., Amasino, R.M., and Krysan, P.J.** (2007). The WiscDsLox T-DNA collection: An Arabidopsis community resource generated by using an improved high-throughput T-DNA sequencing pipeline. *J. Plant Res.* **120**: 157–165.
- Xie, K., Zhang, J., and Yang, Y.** (2014). Genome-wide prediction of highly specific guide RNA spacers for CRISPR–Cas9-mediated genome editing in model plants and major crops. *Mol. Plant* **7**: 923–926.
- Xing, H.-L., Dong, L., Wang, Z.-P., Zhang, H.-Y., Han, C.-Y., Liu, B., Wang, X.-C., and Chen, Q.-J.** (2014). A CRISPR/Cas9 toolkit for multiplex genome editing in plants. *BMC Plant Biol.* **14**: 327.
- Yoo, S.-D., Cho, Y.-H., and Sheen, J.** (2007). Arabidopsis mesophyll protoplasts: A versatile cell system for transient gene expression analysis. *Nat. Protoc.* **2**: 1565–1572.
- Yordanov, Y.S., Regan, S., and Busov, V.** (2010). Members of the LATERAL ORGAN BOUNDARIES DOMAIN transcription factor family are involved in the regulation of secondary growth in *Populus*. *Plant Cell* **22**: 3662–3677.
- Zhang, H., Lin, X., Han, Z., Qu, L.-J., and Chai, J.** (2016). Crystal structure of PXY-TDIF complex reveals a conserved recognition mechanism among CLE peptide-receptor pairs. *Cell Res.* **26**: 543–555.
- Zhang, J., et al.** (2019). Transcriptional regulatory framework for vascular cambium development in Arabidopsis roots. *Nat. Plants* **5**: 1033–1042.
- Zhong, R., Taylor, J.J., and Ye, Z.H.** (1997). Disruption of inter-fascicular fiber differentiation in an Arabidopsis mutant. *Plant Cell* **9**: 2159–2170.
- Zhong, R., and Ye, Z.-H.** (1999). IFL1, a gene regulating inter-fascicular fiber differentiation in Arabidopsis, encodes a homeo-domain-leucine zipper protein. *Plant Cell* **11**: 2139–2152.